COMBINED TOTAL STORM TIDE FREQUENCY ANALYSIS
FOR
DADE COUNTY, FLORIDA

by

R. G. Dean
and
T. Y. Chiu

Sponsored by
Department of Natural Resources
Bureau of Beaches and Shores

Submitted by
Department of Coastal and Oceanographic Engineering
University of Florida
Gainesville, Florida
May, 1981

Table of Contents

List of Figures

I. INTRODUCTION

1.1 Background

In accordance with the objectives and rationale of the Florida Coastal Construction Control Line, the establishment of the line is based on the damage potential of low frequency (100 year) storms. This necessitates the determination of the combined total tides including storm surges, astronomical tide and dynamic wave set-up which occurs primarily inside the wave breaking zone. The objective of the present study which is carried out for Dade County, Florida is to develop, through numerical modeling, valid estimates of the combined total storm tides for return periods of 10, 50, 100, 200 and 500 years.

1.2 Location and General Description of the Study Area

Figure 1 shows the general location of the study area which is on the lower east coast of Florida and is contiguous with Monroe County to the south and Broward County to the north.

The study area consists of about 21.4 miles of Atlantic shoreline in Dade County from the northern county line to the southern end of Key Biscayne. The shoreline of the remaining keys which extends northward from the south county line is not included in the study. The northern 14.5 miles of the study area is the shoreline of the barrier strip which is bisected by Bakers Haulover Inlets at the north and Government Cut at the south. The southern study area is the shorelines of Fisher Island, Virginia Key and Key Biscayne bisected by Norris Cut and Bear Cut. The locality is shown in NOS Chart Nos. 11467, 11466 and 11468 and Figure 1.

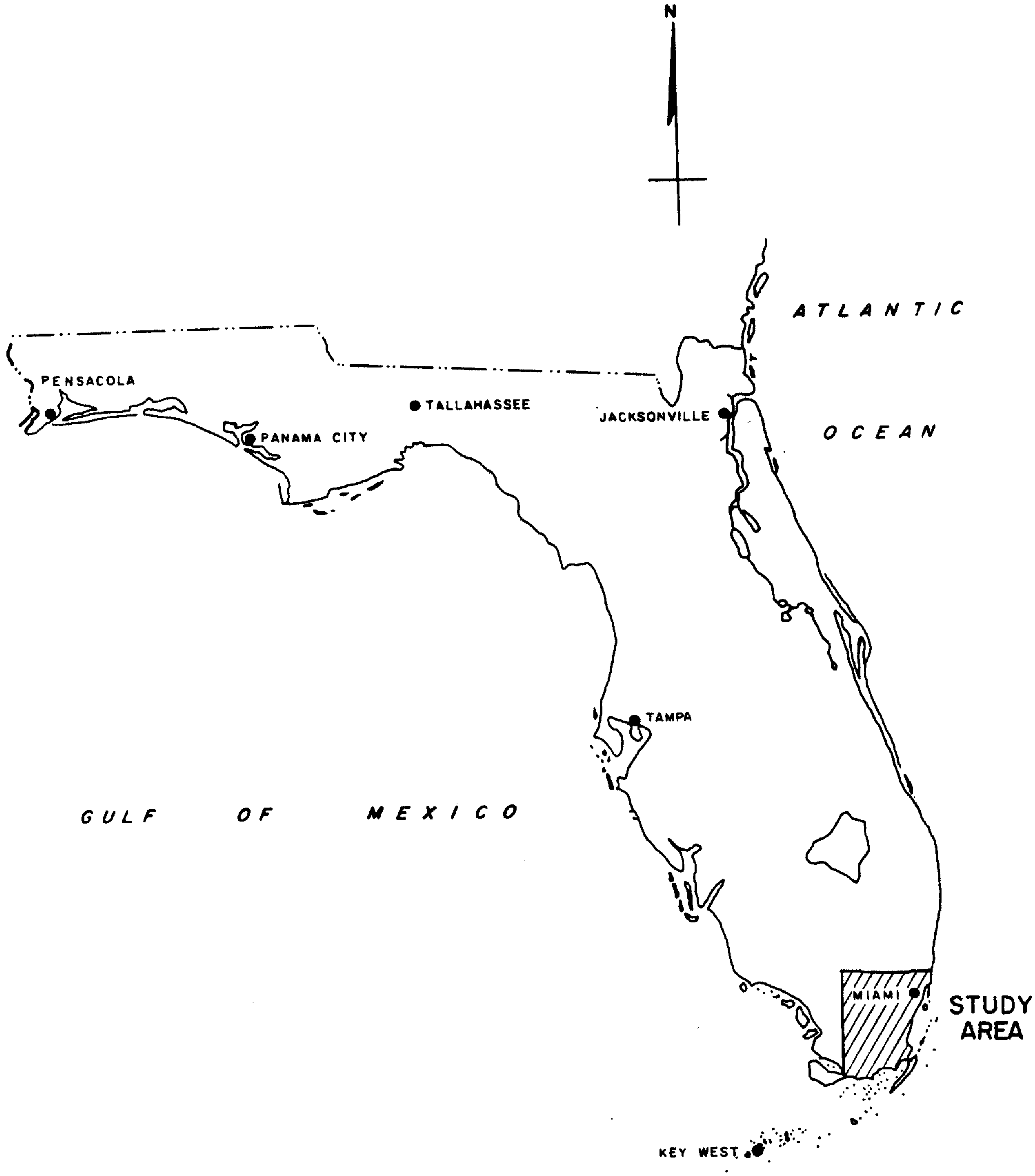

Figure 1. Location Map of Dade County

The northern part of Biscayne Bay separates the barrier strip and islands from Metropolitan Miami on the mainland. The barrier strip occupied by Miami Beach and several other cities varies in width from 0.2 to 1.2 miles. The higher elevations of the barrier strip occur generally along the oceanside; the ground surface slopes downward toward the bay. The average elevation along the oceanside is about 10 ft. Fisher Island, Virginia Key and Key Biscayne are generally low and sandy.

Most of the barrier beach area is highly developed. Miami Beach probably represents the most densely developed resort area of luxury status in the world.

The beaches in Dade County are generally composed of fine sand and shell fragments.

1.3 Scope of the Study

The objective of the study is to develop, verify, and apply a procedure which will yield valid estimates of total storm tides for various return periods at the vicinity of the shoreline in Dade County. Throughout this report, "combined total storm tide" denotes the storm surge due to astronomical tide, wind stress and barometric pressure effects combined with the dynamic wave set-up, the latter occurring dominantly within the wave breaking zone. Available historical hurricane statistics are combined with a numerical model to simulate the storm tides at the site of interest. Storm tide recordings at Miami (Lummus Park) for the hurricanes of September 15-20, 1945 and August 25-September 7, 1979 are employed for model calibration. In addition, surveyed high water levels after the September 6-22, 1926 hurricane are also compared to the computed tide for the same hurricane. Friction characteristics for various types of vegetation, buildings, and underwater areas are developed to represent the actual variation of friction in the model. A simple one-dimensional model is calibrated and used to reduce the cost of computations for a large number of runs simulating a 500-year duration of storm tides. The dynamic wave set-up is based on analytical studies and wave tank tests conducted in conjunction with this study.

II. HISTORICAL PROBABILITIES OF HURRICANE CHARACTERISTICS IN THE AREA OF INTEREST

2.1 Introduction and Data Source

For purposes of calculating the storm tides that occur during a long period, it is necessary to use realistic statistical representations of the important hurricane parameters: p_0 (= central pressure), R (= radius to maximum winds), V_F (= forward speed), θ (= hurricane translation direction), and landfall characteristics. These statistical parameters are based on historical hurricane data as presented in References 1, 2 and 3. In brief, the empirical cumulative probability distributions are plotted for each of the parameters of interest and are then approximated by a series of straight line segments for computer application. All of the parameters are considered to be independent. The following subsections describe the statistical characteristics of the individual parameters of interest.

2.2 Hurricane Frequency and Direction

The hurricanes causing appreciable storm tides in the vicinity of Dade County shoreline are classified as both "landfalling" and "alongshore" storms, depending on their paths relative to the shoreline orientation. Reasonably good data are available describing the characteristics of these storms from approximately 1871 to the present. For purposes of this report, the frequency and direction data contained in References 1, 2 and 3 are merged for a segment of the coast from Long Key to Melbourne Beach within zone 1.

The hurricane direction is defined here as the azimuth of hurricane translation direction at the time of landfall, or, if an alongshore storm, when in close proximity to the site.

The designation of a storm as "landfalling" or "alongshore" is somewhat arbitrary as storms travel over a continuous range of directions and there is no particular direction relative to the shoreline for which the storm-tide generating characteristics change markedly. Moreover, the one directional distribution (Figure 2) is applied for both types of storms. It is important to note that the manner in which the track of a hurricane is characterized for the purposes of this study is different for landfalling and alongshore hurricanes. For landfalling hurricanes, the track is specified by a location of landfall and direction, whereas for the alongshore storms, the track is specified by an offshore distance and a track direction (see Section 2.5).

For purposes here, landfalling hurricanes are considered to be of possible significance if they made landfall within a 200 nautical mile segment of the coast comprising the study area. This segment is centered about the mid-point of the shoreline of Dade County. Table A1 of Reference 3 indicates that the offshore limit of alongshore storms is 70 nautical miles. Figure 3 shows the sectors of propagation paths for alongshore storms.

For purposes of computer use, the cumulative probability distribution is developed from Figure 2 and is presented in Figure 4.

Based on historical data, it is expected that within a 500 year period a total of 280 hurricanes would occur within a distance of 200 nautical miles and that approximately 42% of these would be alongshore storms.

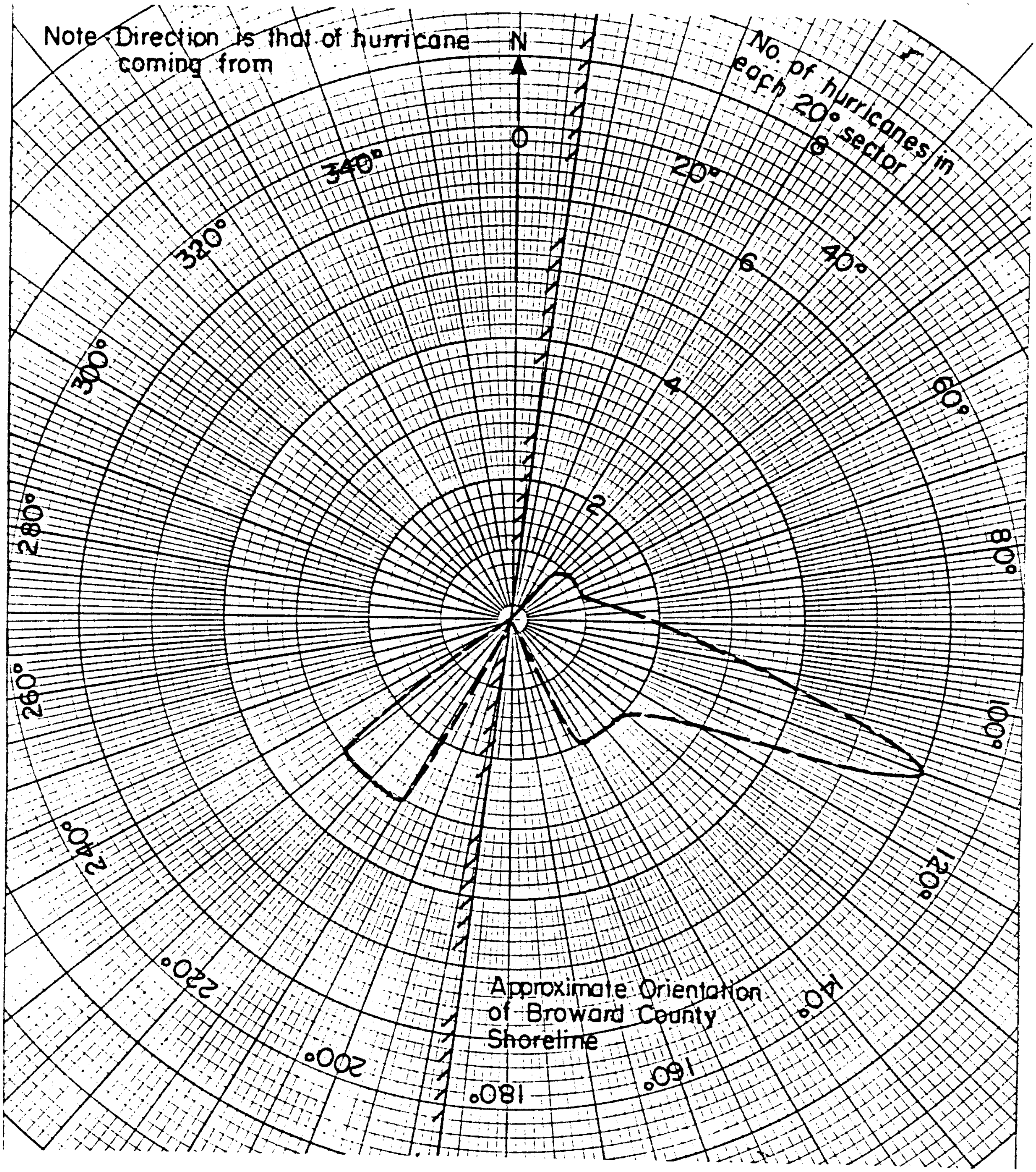

Figure 2. Directional Distribution of Historical Hurricanes Long Key to Melbourne Beach in Zone 1

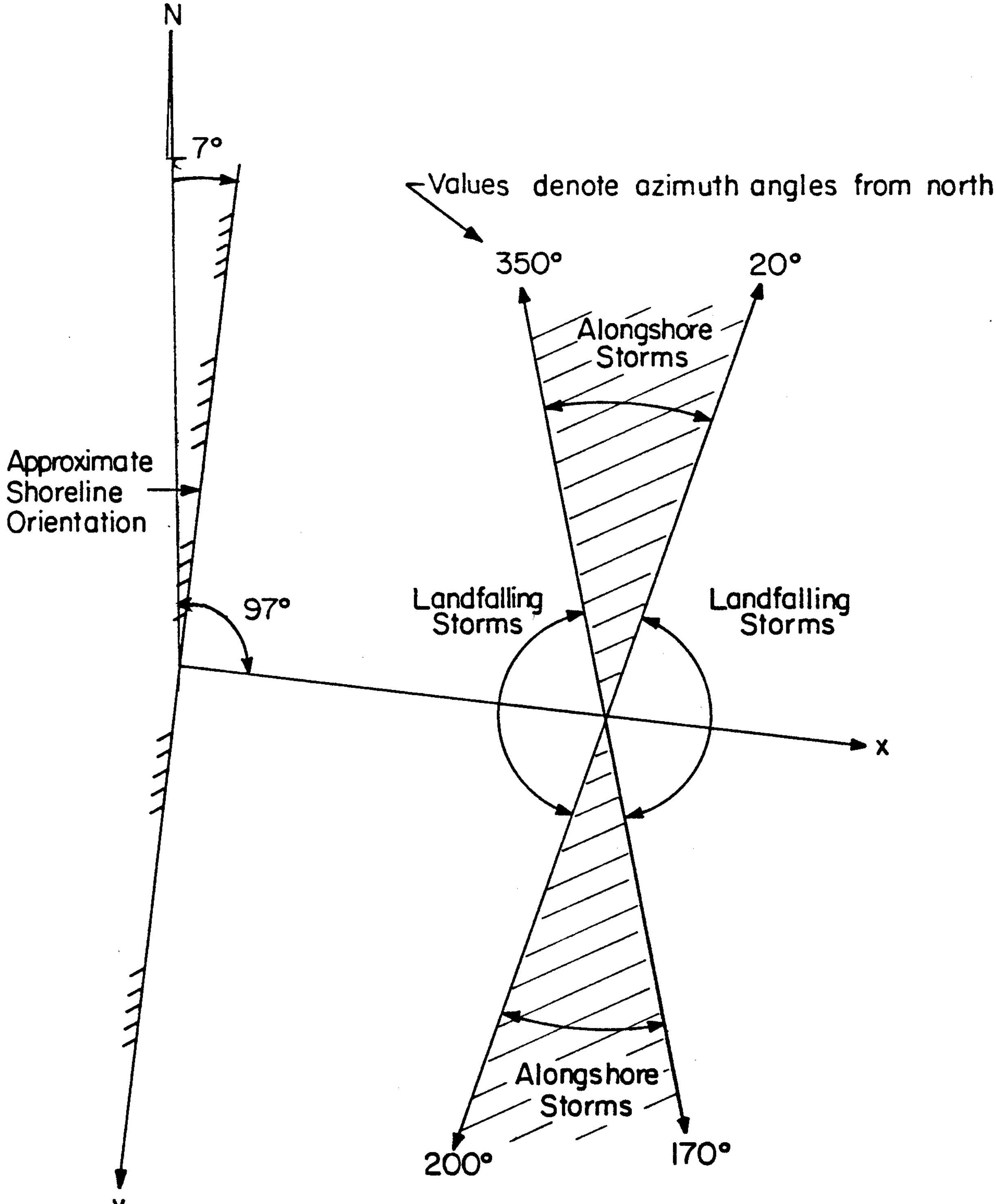

Figure 3. Designation of Alongshore and Landfalling Storms Depending on Track Directions Relative to Shoreline Orientation

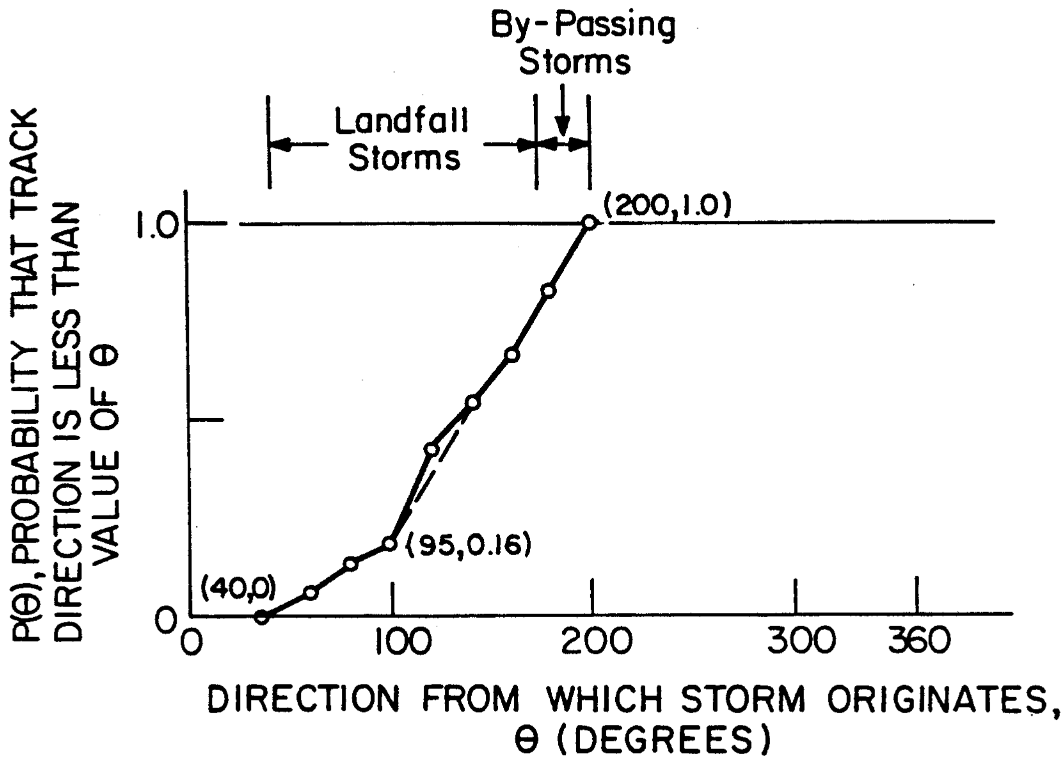

Figure 4. Cumulative Probability Distribution of Storm Track Direction

2.3 Radius to Maximum Winds and Central Pressure Deficit

The statistical descriptions for the radius to maximum winds differ for the landfalling and alongshore storms and are the same for the central pressure deficit. For both types of storms, the statistical representations were based on Table A1 in Reference 3.

Figure 5 presents the cumulative probability distribution of radius to maximum winds for landfalling and exiting storms. Figure 6 shows the cumulative probability distribution of radius to maximum winds for alongshore storms.

The cumulative probability distribution of central pressure deficit for landfalling and alongshore storms is presented in Figure 7.

2.4 Forward Speed

The statistical characteristics of the forward speed of translation of the hurricane systems are found to be the same for the landfalling and alongshore storms. The cumulative probability distributions based on the presentations in Table A1 of Reference 3 are presented in Figure 8 for the landfalling and alongshore storms.

2.5 Track Position

The hurricane track position is established differently for the two types of storms. For the landfalling storms, the position is determined by the y coordinate, Y_F, representing the landfall point. As noted previously, the chance of a hurricane making landfall anywhere along the 200 nautical miles of coast of interest is considered to have equal probability. Figure 9 presents a definition sketch for Y_F and the associated cumulative probability distribution.

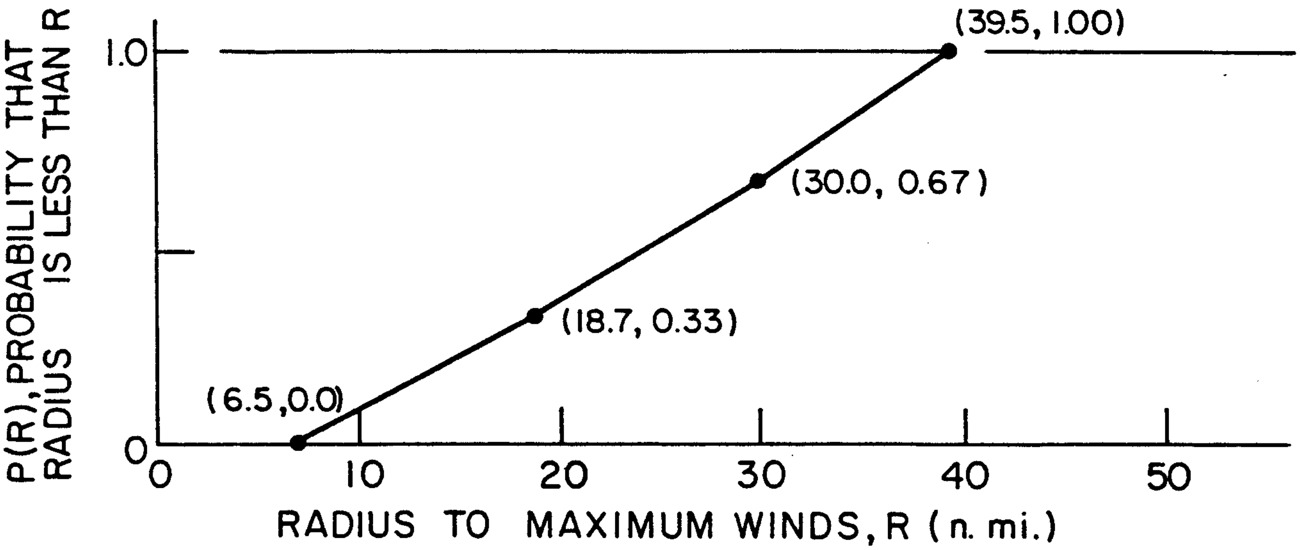

Figure 5. Cumulative Probability Distribution of Radius to Maximum Winds for Landfalling Storms

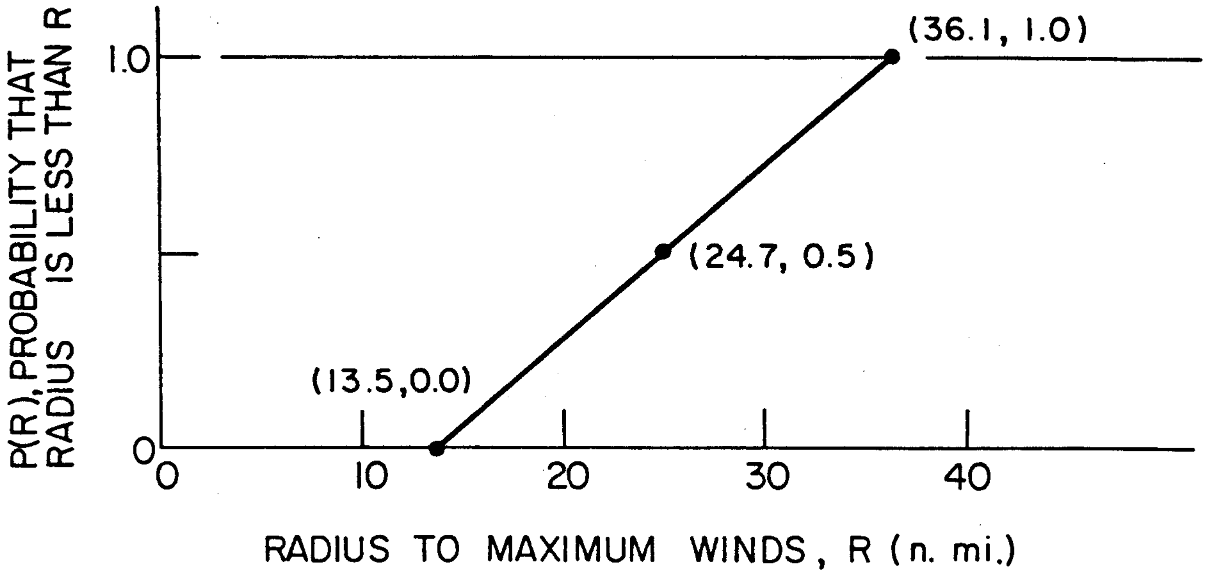

Figure 6. Cumulative Probability Distribution of Radius to Maximum Winds for Alongshore Storms

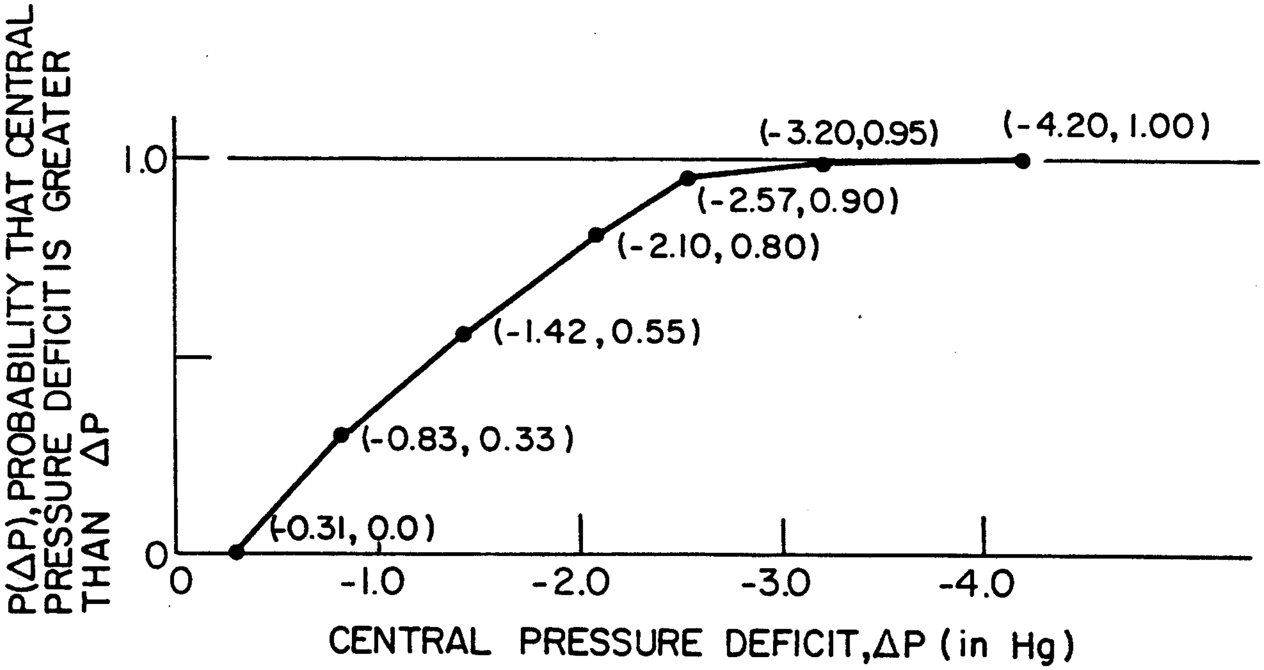

Figure 7. Cumulative Probability Distribution of Central Pressure Deficit, Δp. Landfalling and Alongshore Storms.

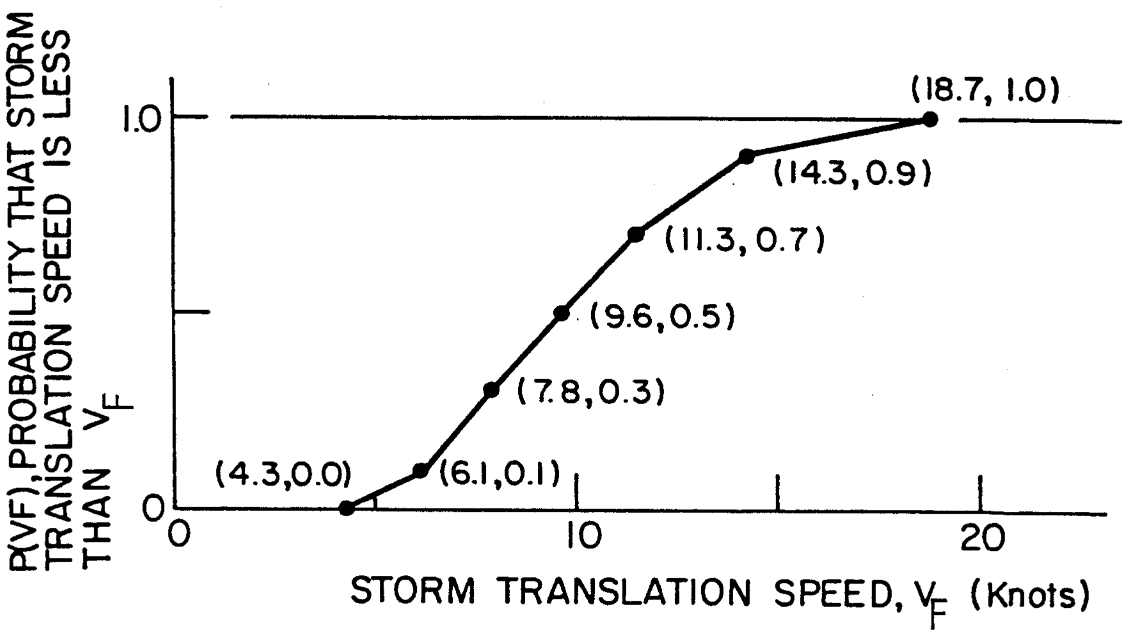

Figure 8. Cumulative Probability Distribution of Storm Translation Speed, V_F. Landfalling and Alongshore Storms.

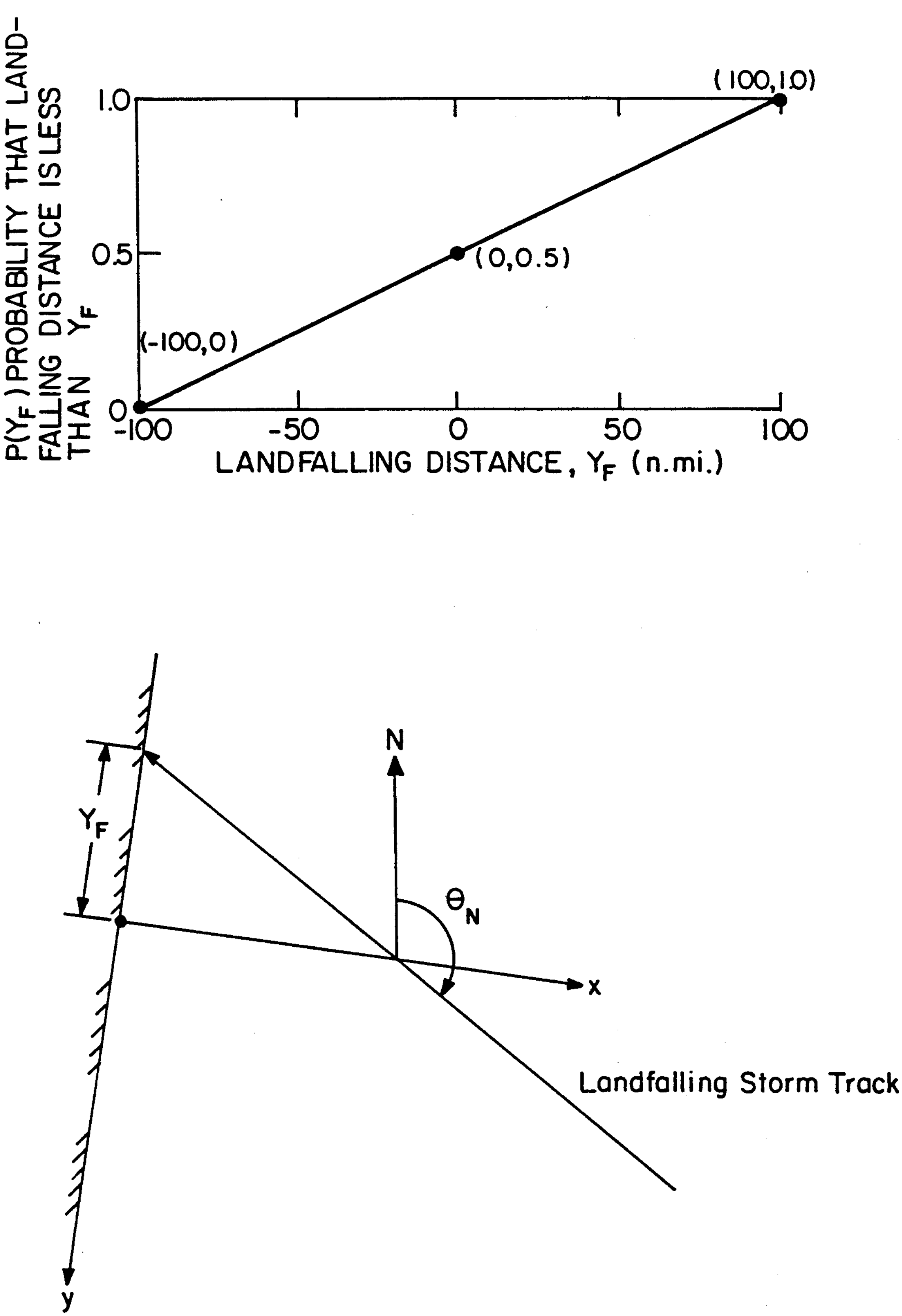

Figure 9. Definition Sketch and Cumulative Probability Distribution of Landfalling Distance, Y_F for Landfalling Storms.

The track position for the alongshore storms is defined by the distance of the track directly offshore from the site. A definition sketch for this variable and the associated cumulative probability distribution is presented in Figure 10.

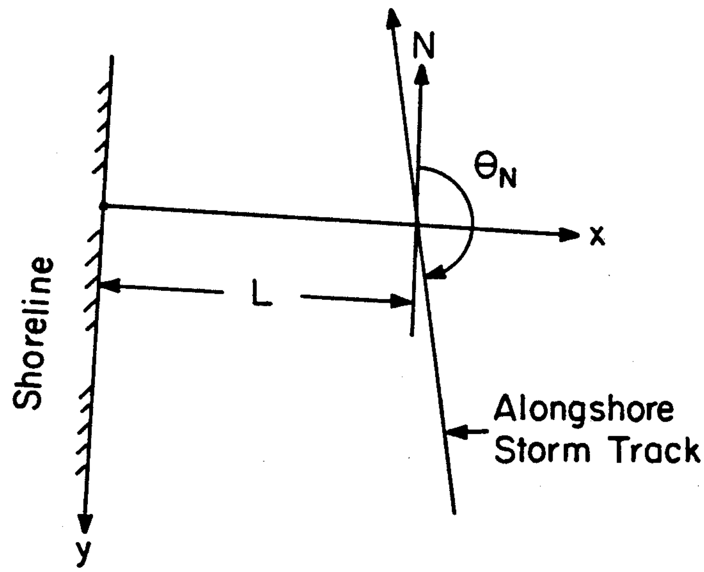

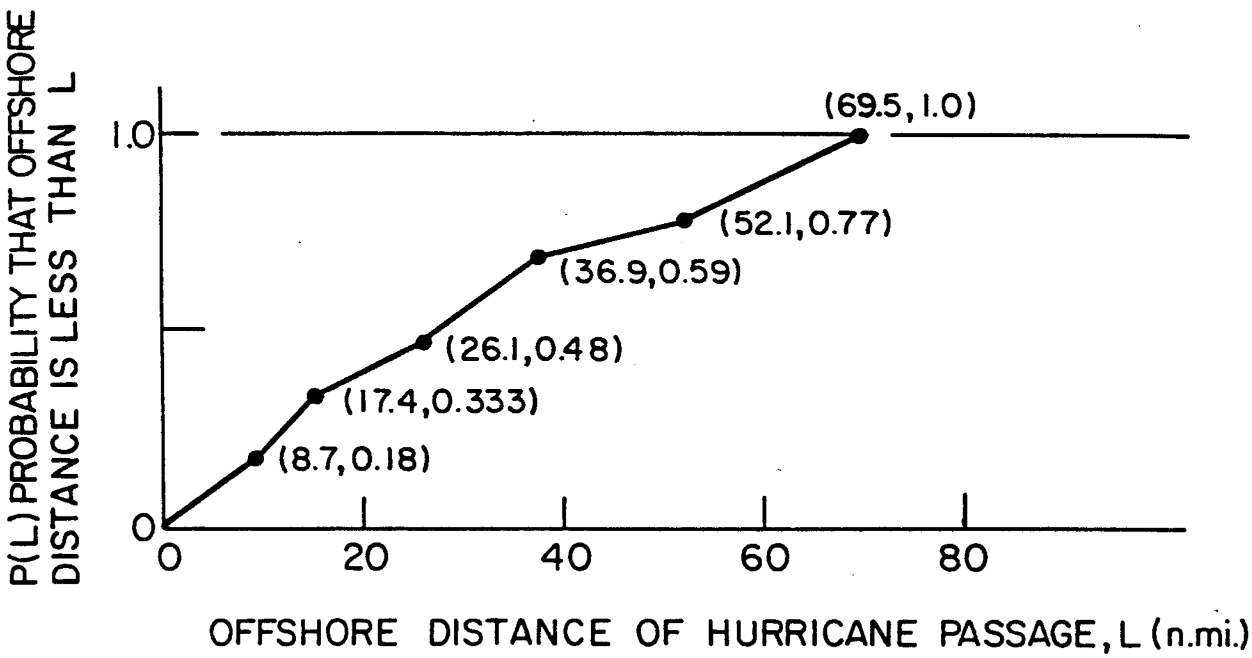

Figure 10. Definition Sketch and Cumulative Probability Distribution of Offshore Distance of Hurricane Passage, L, for Alongshore Storms.

III. METHODOLOGY

3.1 Introduction

This section describes the overall methodology at a very general level to provide the reader with an understanding of the general procedures without addressing the details. The objective of this study is to develop, verify and apply procedures which will yield valid estimates of total storm tides associated with various return periods at the site of interest.

The approach used here is to combine the available historical statistics of hurricanes with a numerical model to simulate the storm tides at the site of interest. Figure 11 is a flow chart illustrating the overall procedure. The numerical model included two-dimensional representations for the offshore area. Prior to its application, the model is verified using tide gage measurements at Miami collected during the September 15-20, 1945 hurricane. The two-dimensional model is significantly more expensive to operate and, since the simulation phase (which generates the statistics of the combined total storm tides) requires the computation of more than one thousand hurricane events, a simpler, far less expensive one-dimensional model is developed and calibrated to yield reasonably good agreement with the predictions of the two-dimensional model. The following sections describe each of the elements in the overall calculation procedure.

3.2 Model Hurricane

The numerical model requires, as input, some representation of the atmospheric pressures and winds which are responsible for the storm tide

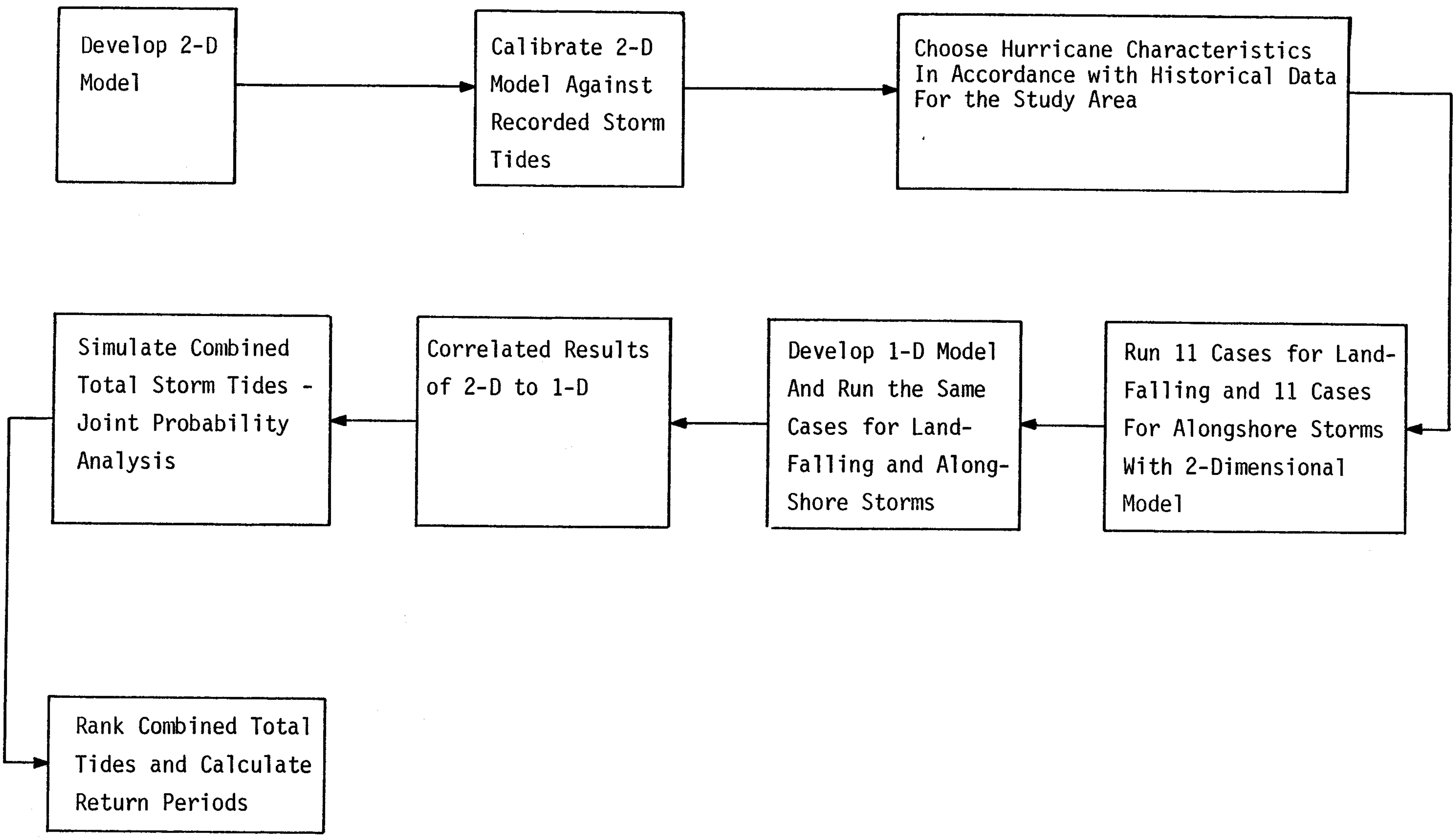

Figure 11. Flow Chart of Methodology

generation. For this purpose, a model hurricane is used which is characterized by the following five parameters:

Δp = Central Pressure Deficit

R = Radius to Maximum Winds

V_F = Speed of Hurricane System Translation

θ = Hurricane Direction

Y_F = Landfall location or some other descriptor of hurricane track.

The model hurricane is one proposed by Wilson (Ref. 4) and is characterized by circular isobars. The associated wind field is determined from a solution of the governing equations of motion. The hurricane model is described in Appendix A.

3.3 Features of the Two-Dimensional Model

The two-dimensional hurricane model is an explicit finite difference system in which the three governing equations are the two horizontal components of the depth-integrated equations of motion and depth-integrated equation of continuity. In principle, the solution is advanced in time as follows. The "staggered" nature of the numerical solution is such that the discharge components at the lines defining each grid are considered fixed for a full time interval, Δt, and the changes in volume in each grid computed and interpreted as changes in water surface elevation, $\Delta\eta$. The time interval, $\Delta t(t^{k-\frac{1}{2}}$ to $t^{k+\frac{1}{2}})$, over which the changes in water level occur is considered to be centered about the time (t^k) that the discharges are considered fixed. Similarly the time interval, $\Delta t(t^k$ to $t^{k+1})$, over which the changes in discharge occur is considered to be centered about the time ($t^{k+\frac{1}{2}}$) that the water levels are considered fixed. The computation of the water level changes is based on the equation of continuity and accounts for the net flux of water onto a grid block. The computation of the two components of discharge is based on the two depth-integrated equations of motion and accounts for the surface (wind) and bottom (friction) shear stresses, the barometric pressure, the Coriolis effect, and the components of slope of the water surface. The model requirements are completed by the specification of appropriate conditions on the boundaries and initial conditions (t=0).

The size of a typical grid of the 2-dimensional model is 2,000 ft x 30,000 ft and the layout of the grid is presented in Figure 12. The conditions specified on the model boundaries include that the water surface diplacements on the boundaries where water is present are equal to the barometric head, due to atmospheric pressure variations. The normal discharge at these boundaries is that required to satisfy the volume requirement by the rising and falling water surface encompassed by the boundaries. Although this is an approximation, if the boundaries are sufficiently distant from the site of interest, any extraneous effects of this approximation should be small. The second type of boundary condition is the no-flow requirement which ensures that the flows are zero normal to grid lines where land elevations exist that are higher than the adjacent water elevations. At times when the elevation of a rising water surface exceeds the land elevation of an adjacent grid block, that block is flooded by a simple algorithm and vice versa for the "deflooding" from grid blocks at times that the falling water surface leaves a block exposed. The effects of bottom vegetation and normally encountered surface friction factors are accounted for in the model in an approximate manner.

3.4 Features of the One-Dimensional Model

As noted earlier, a simple one-dimensional numerical model was developed and calibrated to allow the statistics to be generated based on simulation (calculations) of many storms and associated storm surges.

The one-dimensional numerical model is described as follows.
A transect line is established along a line which is approximately perpendicular to the bottom contours. The characteristics (Δp, R, θ, V_F and track) of the hurricane are defined and the hurricane is advanced along

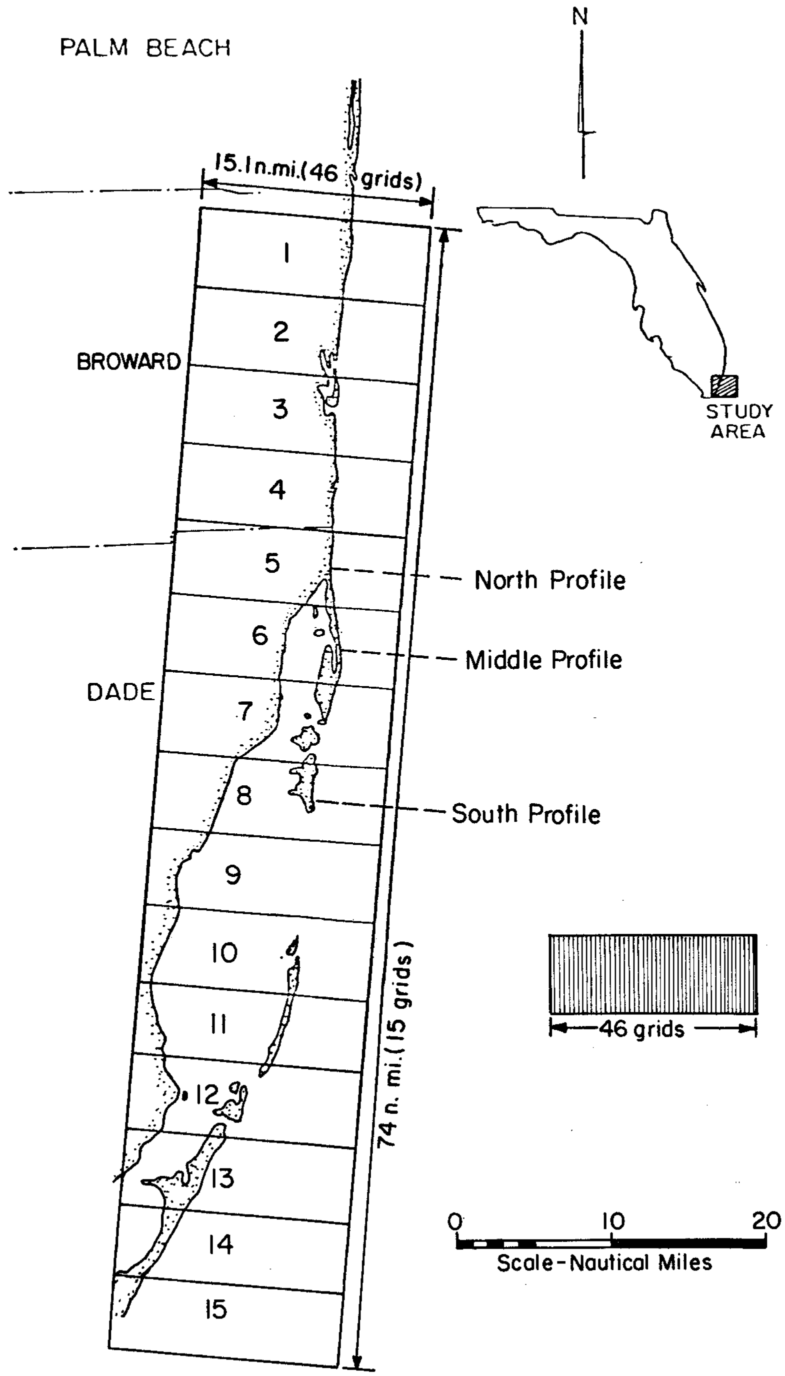

Figure 12. Grid System Used in the Two-Dimensional Numerical Model of Storm Surges for Dade County

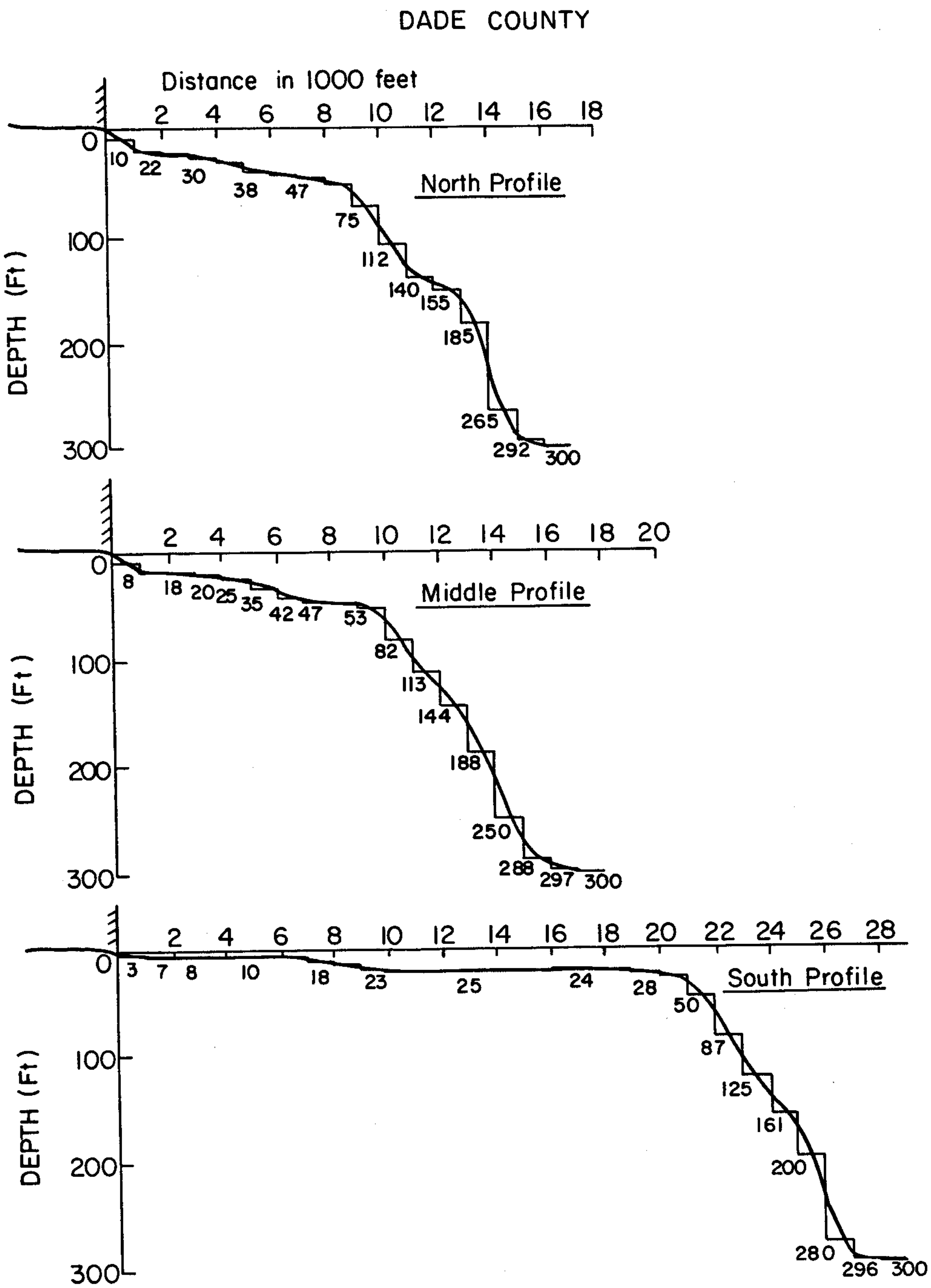

Figure 13. Locations of and Approximations to the Three Dade County Profiles Selected for the Study

the transect line. The water surface displacement (boundary condition) at the seaward end of the transect line is taken as the static response of the water surface to the barometric pressure deviation at that point.

3.5 Application of Numerical Models

The various numerical models were applied in four different phases:

1) Verification of the two-dimensional numerical model against tide gage records at Miami obtained during the 1945 and 1979 hurricanes as reported in Reference 5 and National Ocean Survey tide recordings.
2) Based on the characteristics of historical hurricanes, the two-dimensional model was run for 11 landfalling storms and 11 alongshore storms with characteristics representative of the more probable and significant storms,
3) The one-dimensional model was run for the same 22 storms described in 2) above. The storm tides developed in 2) then serve as a basis for adjusting the output of the one-dimensional model during the simulation phase.

3.6 Simulation of an n-Year Sequence of Hurricane Associated Storm Tides

With the statistical characteristics of historical hurricanes available and the simple one-dimensional model calibrated as described in the preceding section, the simulation shown in Figure 14 was carried out. The first phase of the simulation comprises the selection of the hurricane characteristics in accordance with the historical data. In each storm, this involves the following:

1) Quantifying Δp, R, V_F, θ and hurricane track in accordance with the historical probabilities (as will be noted later, the details of this step differ somewhat for the landfalling and alongshore storms),

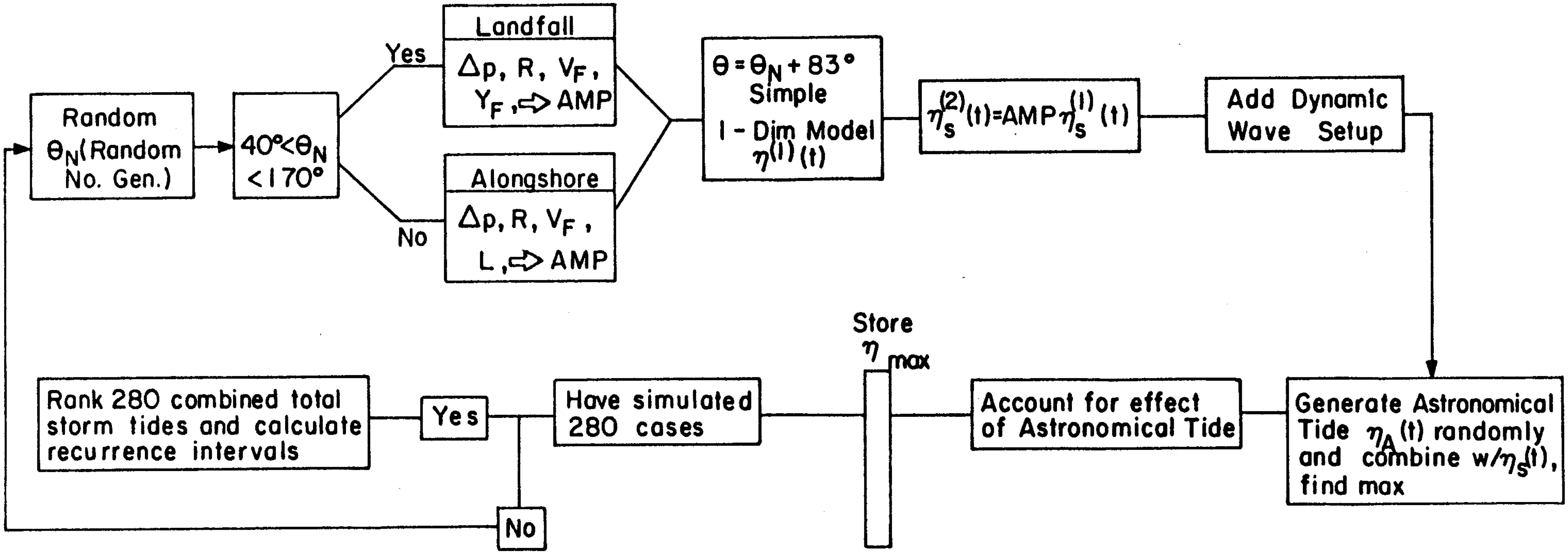

Figure 14. Flow Chart for Storm Tide Simulations (After Calibration to Determine $(AMP)_{LF}$ and $(AMP)_{ALONG}$)

2) For these characteristics, the one-dimensional numerical model is run to determine the storm surge at the site of interest. This storm surge is then adjusted in accordance with the factors obtained from the two-dimensional model calibration runs,

3) For the landward grid and each time step, the contribution due to dynamic wave set-up is included,

4) Using predicted astronomical tides during the hurricane season, the relative time of occurrence of the hurricane is generated and a combined total tide as the sum of the astronomical tide and total storm surge is obtained.

5) Determine whether enough storms have been simulated for the n-year simulation. For example, the hurricane statistics indicate that within a period of 500 years, there should be 280 storms (161 landfalling and 119 alongshore storms) which affect the shoreline within a distance of 200 nautical miles.

6) After the required number of storms and associated storm tides have been simulated, the peak water levels for each storm are ranked and the return period, TR, is calculated, according to

$$TR = \frac{500}{M}$$

where M is the rank of the combined total tide level. (For example if the simulation was carried out for a 500 year period, the highest combined total tide level would have a return period of 500 years, the second highest water level would have a return period of 250 years, etc.). Finally, by presenting these results on semi-log paper, it is possible to interpolate to return periods of interest, i.e., TR = 10, 50, 100 and 500 years, yield the final results.

IV. NUMERICAL MODELS-DESCRIPTION AND CALIBRATION

As noted in the previous chapter the methodology includes the development, calibration and application of a series of numerical models and statistical hurricane characteristics to the simulation of a long period (500 years) to establish combined total tide levels associated with various return periods of interest. Figure 11 presents a flow chart of the methodology. This chapter parallels that of Chapter III; however, much greater detail is presented. The following subsection reviews the various numerical models and calibration or calculation procedures.

4.1 Numerical Models -

Two-Dimensional Numerical Model - The grid system associated with this numerical model relative to the shoreline is presented in Figure 12. Each grid is 2,000 ft. x 30,000 ft. and the purpose of the numerical model is to calculate the storm surges as the hurricane translates across the shelf.

Governing Differential Equations - The governing differential equations for the two-dimensional model include the equation of continuity and the two depth-integrated approximate momentum equations, given by:

$$\frac{\partial \eta}{\partial t} + \frac{\partial q_x}{\partial x} + \frac{\partial q_y}{\partial y} = 0 \quad (1)$$

$$\frac{\partial q_x}{\partial t} = -gh\,\frac{\partial \eta}{\partial x} - \frac{h}{\rho}\frac{\partial p_\eta}{\partial x} + \frac{\tau_{w_x}}{\rho} - \frac{\tau_{b_x}}{\rho} - \beta q_y \quad (2)$$

$$\frac{\partial q_y}{\partial t} = -gh\,\frac{\partial \eta}{\partial y} - \frac{h}{\rho}\frac{\partial p_\eta}{\partial y} + \frac{\tau_{w_y}}{\rho} - \frac{\tau_{b_y}}{\rho} + \beta q_x \quad (3)$$

where x, y = horizontal coordinate directions

t = time coordinate

η = displacement of water surface from a horizontal reference

q_x, q_y = discharge components per unit width in the x and y directions

h = total water depth including water surface displacement

g = acceleration of gravity

$\tau_{w_{x,y}}$ = wind stress components in the x and y directions

$\tau_{b_{x,y}}$ = bottom stress in the x and y directions

$p\eta$ = barometric pressure

β = Coriolis parameter = $2\Omega \sin\phi$

Ω = rate of earth's angular rotation

ϕ = latitude of site of interest.

The surface and bottom shear stress components are related to the wind speed W and discharge components by

$$\tau_{w_{x,y}} = \rho K \, W W_{x,y} \tag{4}$$

$$\tau_{b_{x,y}} = \rho \frac{f}{8} \frac{|q| \, q_{x,y}}{h^2} \tag{5}$$

$$|q| = \sqrt{q_x^2 + q_y^2}$$

in which K is an air-sea friction coefficient developed by Van Dorn (Ref. 6); and depends on the wind speed as follows:

$$K = \begin{cases} 1.1 \times 10^{-6} & \text{for } W < W_{cr} \\ 1.1 \times 10^{-6} + 2.5 \times 10^{-6} \left(1 - \frac{W_{cr}}{W}\right)^2 & \text{for } W \geq W_{cr} \end{cases} \tag{6}$$

where W_{cr} = 23.6 ft/sec

The quantity, f, is the Darcy-Weisbach bottom friction coefficient and varies with depth, bottom roughness and vegetation, if present. For purposes of this study, f was developed by Christensen and Walton (Ref. 7) of the University of Florida and is presented in Figure 15.

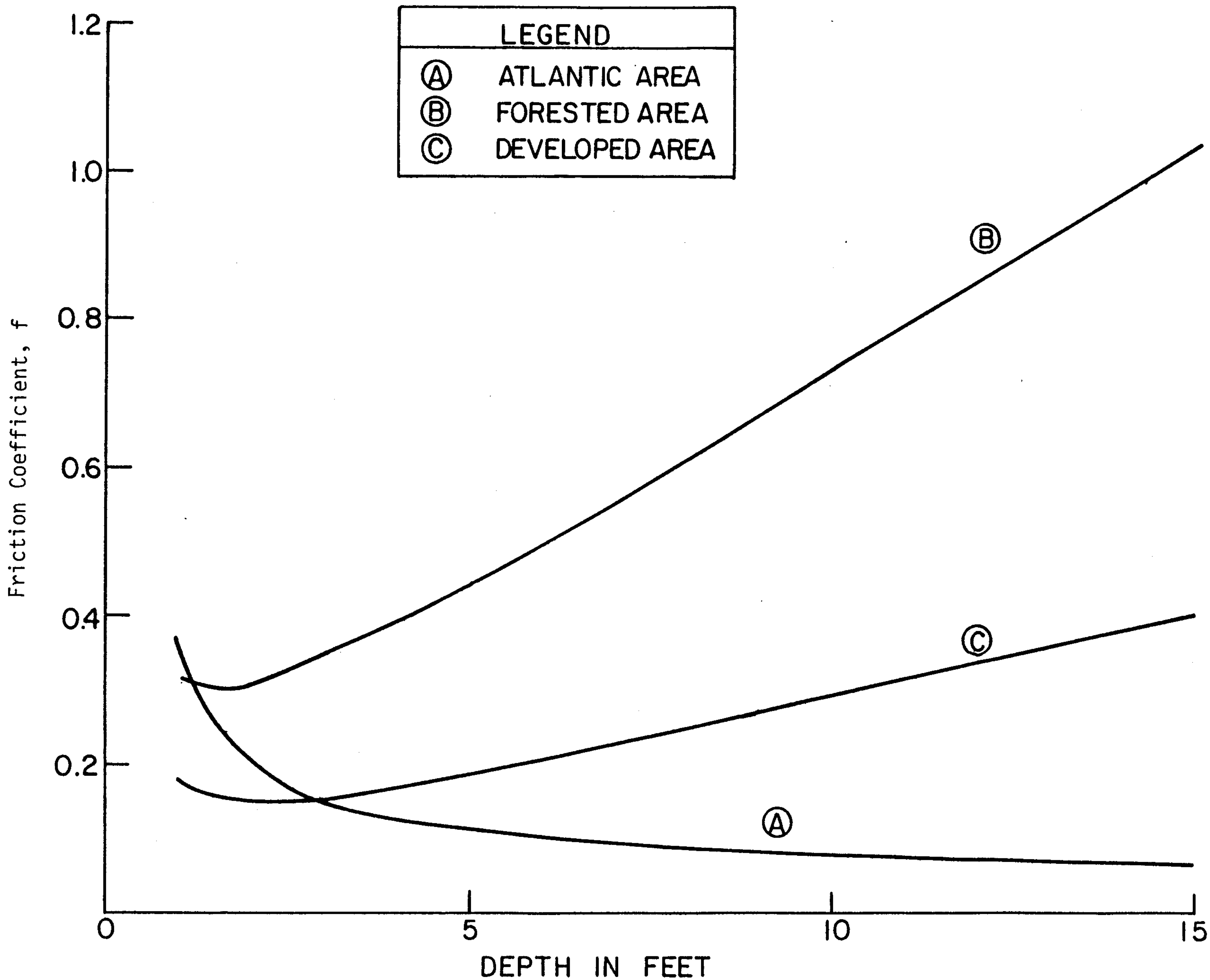

Figure 15. Bottom Friction Coefficients for Various Bottom Conditions Encountered in the Study Area

Finite Difference Forms of Governing Differential Equations - The finite difference representations of Equations (1), (2), and (3) are expressed as follows in preparation for an explicit type of solution:

$$\eta_{i,j}^{k+\frac{1}{2}} = \eta_{i,j}^{k-\frac{1}{2}} - \Delta t \left[\frac{q_{x_{i+1,j}}^{k} - q_{x_{i,j}}^{k}}{\Delta x} + \frac{q_{y_{i,j+1}}^{k} - q_{y_{i,j}}^{k}}{\Delta y} \right] \tag{7}$$

$$q_{x_{i,j}}^{k+1} = \frac{1}{A_x^k} \left\{ q_{x_{i,j}}^{k} + \left[\frac{\tau_{w_x}}{\rho} - g\bar{h}_x \left(\frac{\eta_{i,j}^{k+\frac{1}{2}} - \eta_{i-1,j}^{k+\frac{1}{2}}}{\Delta x} \right) - \frac{\bar{h}_x}{\rho} \left(\frac{p_{i,j}^{k+\frac{1}{2}} - p_{i-1,j}^{k+\frac{1}{2}}}{\Delta x} \right) - \beta \overline{q_{y_{i,j}}^{k}} \right] \Delta t \right\} \tag{8}$$

$$q_{y_{i,j}}^{k+1} = \frac{1}{A_y^k} \left\{ q_{y_{i,j}}^{k} + \left[\frac{\tau_{w_y}}{\rho} - g\bar{h}_y \left(\frac{\eta_{i,j}^{k+\frac{1}{2}} - \eta_{i,j-1}^{k+\frac{1}{2}}}{\Delta y} \right) - \frac{\bar{h}_y}{\rho} \left(\frac{p_{i,j}^{k+\frac{1}{2}} - p_{i,j-1}^{k+\frac{1}{2}}}{\Delta y} \right) + \beta \overline{q_{x_{i,j}}^{k}} \right] \Delta t \right\} \tag{9}$$

in which the superscripts (k) denote times and subscripts (i,j) denote horizontal grid locations (x,y), respectively,

$$A_{x,y}^{k} = 1 + \frac{\rho f |q^k|}{8(\bar{h}_{x,y})^2} \tag{10}$$

$$\overline{q_{y_{i,j}}^{k}} = \frac{1}{4} \left[q_{y_{i,j}}^{k} + q_{y_{i,j+1}}^{k} + q_{y_{i-1,j}}^{k} + q_{y_{i-1,j+1}}^{k} \right] \tag{11}$$

$$\overline{q_{x_{i,j}}^{k}} = \frac{1}{4} \left[q_{x_{i,j}}^{k} + q_{x_{i+1,j}}^{k} + q_{x_{i,j-1}}^{k} + q_{x_{i+1,j-1}}^{k} \right] \tag{12}$$

and

$$\bar{h}_x = \frac{1}{2} \left[h_{i,j}^{k+\frac{1}{2}} + h_{i-1,j}^{k+\frac{1}{2}} \right] \tag{13}$$

$$\bar{h}_y = \frac{1}{2} \left[h_{i,j}^{k+\frac{1}{2}} + h_{i,j-1}^{k+\frac{1}{2}} \right] \tag{14}$$

$$|q^k| = \sqrt{ \left(\overline{q_{x_{i,j}}^{k}} \right)^2 + \left(\overline{q_{y_{i,j}}^{k}} \right)^2 } \tag{15}$$

4.2 Boundary Conditions

To complete formulation of the problem, boundary conditions must be specified at the boundaries of the grid presented in Figure 12. On the "open" (water) boundaries, the water surface is specified to be that associated with the barometric pressure, i.e.

$$\eta_{B_{i,j}} = \left(\frac{p_\infty - p_{i,j}}{\rho g}\right) \tag{16}$$

in which p_∞ denotes the far field barometric pressure. In addition, on the open boundary grid cells, it is specified that only discharge components perpendicular to the boundaries occur and that these discharges on the exterior boundaries of the grid system are those required to satisfy the continuity equation (Eq. 7).

On the "closed" boundaries, i.e., at the shoreline where land elevations are higher than the adjacent water elevations, a no-flow boundary condition is specified perpendicular to that boundary. However, "flooding" and "deflooding" of grid blocks adjacent to the boundaries can occur. Flooding occurs when the water level is greater by a specified small amount than the ground elevation of an adjacent grid block. When this condition exists, the grid block is activated by a simple allocation of this excess elevation on the newly activated block and in subsequent time steps the grid block is incorporated into the normal calculation scheme. Deflooding occurs when the water level on a grid block drops below a specified level leaving a very small depth on that block. The block is "deactivated" and the excess water placed on the adjacent grid.

4.3 Solution

The solution is started from an initial condition of zero water surface displacement and zero discharge components. The hurricane system is translated along a specified path at a designated speed. At each time step, the hurricane effects (represented by the pressure and wind stress components) on each cell are calculated and the finite-difference equations (Eqs. 7, 8 and 9) employed. The results are updated values of η, q_x and q_y for each cell. It is noted that the system of finite difference equations employed here are explicit and they are staggered in space and time. In principle the discharges are considered fixed from $t_{k-\frac{1}{2}}$ to $t_{k+\frac{1}{2}}$ and the change in water levels evaluated (Eq. 7). The water levels are then considered fixed from t_k to t_{k+1} and updated discharge components determined (Eqs. 8 and 9). The spatial staggered nature of the system is due to η being defined at the center of each grid and q_x and q_y on the boundaries of the grid.

One-Dimensional Numerical Model - The one-dimensional numerical model is significantly less expensive and simpler to run and is used in the simulation phase, in order to generate the required data within budgetary constraints. The justification for using the one-dimensional model is that it can be adequately calibrated with the rather complete two-dimensional model.

The one-dimensional numerical model is a static model and therefore no effects of inertia or friction are included. The (single) governing equation expressed in finite difference form is:

$$\eta_{i+1} = \eta_i + \frac{\tau_{w_x}}{\rho g\bar{h}} - \left(\frac{p_{i+1} - p_i}{\rho g}\right) \Delta x \tag{17}$$

in which p and τ_{w_x} are the barometric pressure and wind stress along the transect line perpendicular to shore and passing through the site.

The seaward boundary condition is that the water surface displacement is

$$\eta_i = \frac{p_\infty - p_i}{\rho g} \tag{18}$$

In applying the one-dimensional numerical model, a fairly coarse grid (1,000 ft.) is used as presented in Figure 13.

4.4 Simulation

To summarize information presented earlier, this phase includes the simulation of the occurrence of 500 years of hurricanes along a shoreline segment of 200 nautical miles. In an average 500 year period, there would be a total of 280 hurricanes with 161 "landfalling" storms and 119 "alongshore" storms.

Selection of Hurricane Parameters - Each of the five idealized hurricane parameters (Radius to Maximum Winds, R; Central Pressure, p_0, (or Central Pressure Deficit, Δp); Track Direction, θ; System Forward Speed, V_F; and Track Position, (Y_F for landfalling storms, and X_L for alongshore storms) is determined randomly in accordance with the associated cumulative probability functions. The procedure is described below for the track direction, θ, and is similar for all other variables.

The approximate piece-wise linear cumulative distribution function for track direction, θ, is shown in Figure 4. The nature of this function is such that the more predominant directions are those where the function rises steeply. To randomly select a track direction in accordance with this distribution function, the computer first generates a random number between 0 and 1 corresponding to the cumulative probability. Suppose that this number is 0.38. Since this value corresponds to the linear segment between directions of 95^o and 200^o, the computer interpolates to find a track direction, θ, of 122.5^o. We note that this is a landfalling storm. The other four parameters are determined similarly with a separate and independent random number being generated for each parameter and the appropriate cumulative probability distribution used, depending on whether the storm is landfalling or an alongshore storm.

Calculation of Storm Tide at Site of Interest - With the hurricane parameters established, the calibrated simple one-dimensional model is employed to calculate the storm tide history at the site of interest.

Dynamic Wave Set-Up - When waves break, a shoreward directed force in addition to the wind stress, is exerted on the water in the surf zone. This causes an additional rise in water level termed "wave set-up." This effect has been studied extensively in the laboratory (Saville (Ref. 8), Bowen and Simmons (Ref. 9)) and tide gage measurements during severe storms have confirmed its importance in nature. Most of the information relative to wave set-up has been developed for "regular" waves, that is for a wave train in which each wave is the same as the preceding wave. Waves in nature, however, are not regular and tend to occur in groups. A recent analytic study by Lo (Ref. 10) has shown that for natural wave trains there is a dynamic wave set-up that is approximately 50% larger than would be predicted by a static treatment. In order to evaluate this result, model studies were conducted in the large University of Florida wave tank. It was found that the experimental and analytical results by Lo were in approximate agreement.

The maximum dynamic wave set-up, η'_{max} across the surf zone can be shown to be approximately

$$\eta'_{max} = 0.22\ H_b \qquad (19)$$

which includes the dynamic factor of 50% and in which H_b is the breaking wave height based on the deep water significant wave height, H_o, taken approximately as

$$H_b = 0.94\ H_o \qquad (20)$$

The deepwater significant wave height is determined from an extension of a method recommended for hurricane generated waves as summarized in the Shore Protection Manual (Ref. 11),

$$(H_o)_{max} = 16.5\ e^{R(\Delta p/100)}\ (1 + \frac{0.208\ V_F}{\sqrt{U_R}}) \qquad (21)$$

where R = radius of maximum winds in nautical miles, Δp = central pressure deficit in inches of mercury, V_F = translation speed of hurricane in knots, and U_R = maximum sustained wind speed in knots. For purposes here the local effective deep water significant wave height is based on the local winds, U, at the surf zone area of interest and the maximum winds in the hurricane, U_{max} as

$$H_o = (H_o)_{max} \left(\frac{U}{U_{max}}\right)^2 \tag{22}$$

Equations 19, 20, 21 and 22 provide the basis for determining the maximum dynamic wave set-up within the surf zone. The computed value of η'_{max} was added to the nearshore storm surge. It is stressed that η'_{max} represents the maximum dynamic wave set-up across the surf zone and that this value varies with time (since the wind speed varies with time). The value of η'_{max} was computed at each time step for the shoreward grid, and added to the corresponding surge value resulting from wind stress and barometric pressure as described in the previous sections.

Combination of Storm Surge and Astronomical Tide - A particular hurricane can be "phased" such that the maximum resulting storm surge is increased or decreased by astronomical tidal fluctuations. Considering the predicted astronomical tidal fluctuations from June 1 to November 30, 1974, to be representative of those occurring during the hurricane season and assuming the phasing of hurricane occurrence and astronomical tides to be independent, the combination of these tidal components was carried out in the following manner. Following the calculation of a total storm surge history for a particular simulated hurricane, a starting time for the hurricane is selected randomly between June 1 and November 30, 1974 by the method described earlier. With the total storm surge history thus phased with the astronomical tide, it is a simple matter to search in the computer to determine the maximum of the combined total storm surge and astronomical tide.

4.5 Computation of Return Periods

With a sufficient number (280) of maximum combined total storm tides simulated to represent a typical 500 year time interval, the tides associated with various return periods of interest are determined. The 280 maximum combined total storm tides were ranked in descending order with the largest occurring first. The return period, TR, of the ranked tides is then

$$TR = \frac{500}{M} \tag{22}$$

in which

TR = Return period in years between expected exceedances of the associated maximum storm tide

M = Rank of maximum storm tide

As an example, for M = 280 (associated with the lowest water level) the return period would be:

$$TR_{280} = \frac{500}{280} = 1.79 \text{ years}$$

which is reasonable since records indicate that there is approximately one hurricane every 2 years, and the smallest storm tide could be expected to be exceeded approximately once every 2 years. As a second example, the return period for M = 1 (associated with the highest water level) is

$$TR_1 = \frac{500}{1} = 500 \text{ years}$$

The ranked maximum total storm tide and associated return periods can be plotted and the storm surge associated with any return period determined.

Finally, it is noted that it is possible to run the simulation procedure any number of times to determine the stability (constancy) of any total storm tide associated with a given return period. It is expected that for a 500 year simulation, the storm tides associated with the longer (> 200 year) return periods would not be well-defined by one simulation and would exhibit variation from simulation to simulation. However, the storm surges associated with the lower return periods (TR < 100 years) should be well-defined by a 500 year simulation and hence are not expected to vary significantly for various simulations.

V. CALIBRATION AND RESULTS

5.1 Rationale

Ideally there are sufficient storm tide data (from tide gages) at a site of interest to allow calibration of the numerical model. If this is the case, then it would be possible to calibrate the one-dimensional numerical model with data from the site and it would not be necessary to utilize the two-dimensional model described earlier. Unfortunately, there are insufficient tide measurements at the site; and it is therefore necessary to utilize the two-dimensional model as an intermediate representation.

The calibration procedure followed is, first, to validate/calibrate the two-dimensional numerical model using the tide gage data at Miami Beach (Recreation Pier) for the 1945 and 1979 hurricanes. After these calibrations/validations, a check run was made to compute the storm tide of the 1926 hurricane and compare it with the high water levels measured after the storm in Miami Beach area. With these calibrations as a basis for the two-dimensional model it is then run for a series of storms with parameters encompassing representative ranges. These include 11 land-falling and 11 alongshore storms to determine the peak storm surges at the site. These results are then utilized to calibrate the one-dimensional numerical model which is run for the same 22 hurricane conditions.

5.2 Results--Calibration of Two-Dimensional Numerical Model

A tide gage recording of the September 15-20, 1945 hurricane tide at Miami Beach (Recreation Pier) is presented by Harris (Ref. 5). A portion of the tidal record encompassing the peak tide for this storm is presented in Figure 16. Figure 17 shows the peak portion of the measured tide in Figure 16. The tide gage recording of the August 25-September 7, 1979 hurricane tide at Miami Beach (Recreation Pier) is presented in Figure 18 from data provided by National Ocean Survey. Reference 12 gives the measured high water levels caused by the September 17-21, 1926 hurricane in the Miami Beach area. The range of the measured high water levels and its mean value are presented in Figure 19. The characteristics of these hurricanes are presented in Table I. The two-dimensional numerical model is run for the characteristics presented in Table I and the results are compared with the measurements in Figures 17, 18 and 19. It is seen that the calculated storm tide peaks are within 0.12 ft of the measured storm tide peaks. The calibration for the two-dimensional model is thus taken as 1.0, i.e., the calculated storm tides do not have to be adjusted.

TABLE I
Characteristics of Hurricanes

	September 15-20, 1945	August 25-September 7, 1979	September 6-22, 1926
Δp (in. Hg)	- 1.84	- 1.28	- 2.33
R (n. mi.)	24.0	22.0	24.0
V_F (knots)	10.0	-10.0	16.0
θ (degrees)	130.0	165.0	113.5
Y_F (n. mi.)	73.0		73.0
L (n. mi.)		45.0	

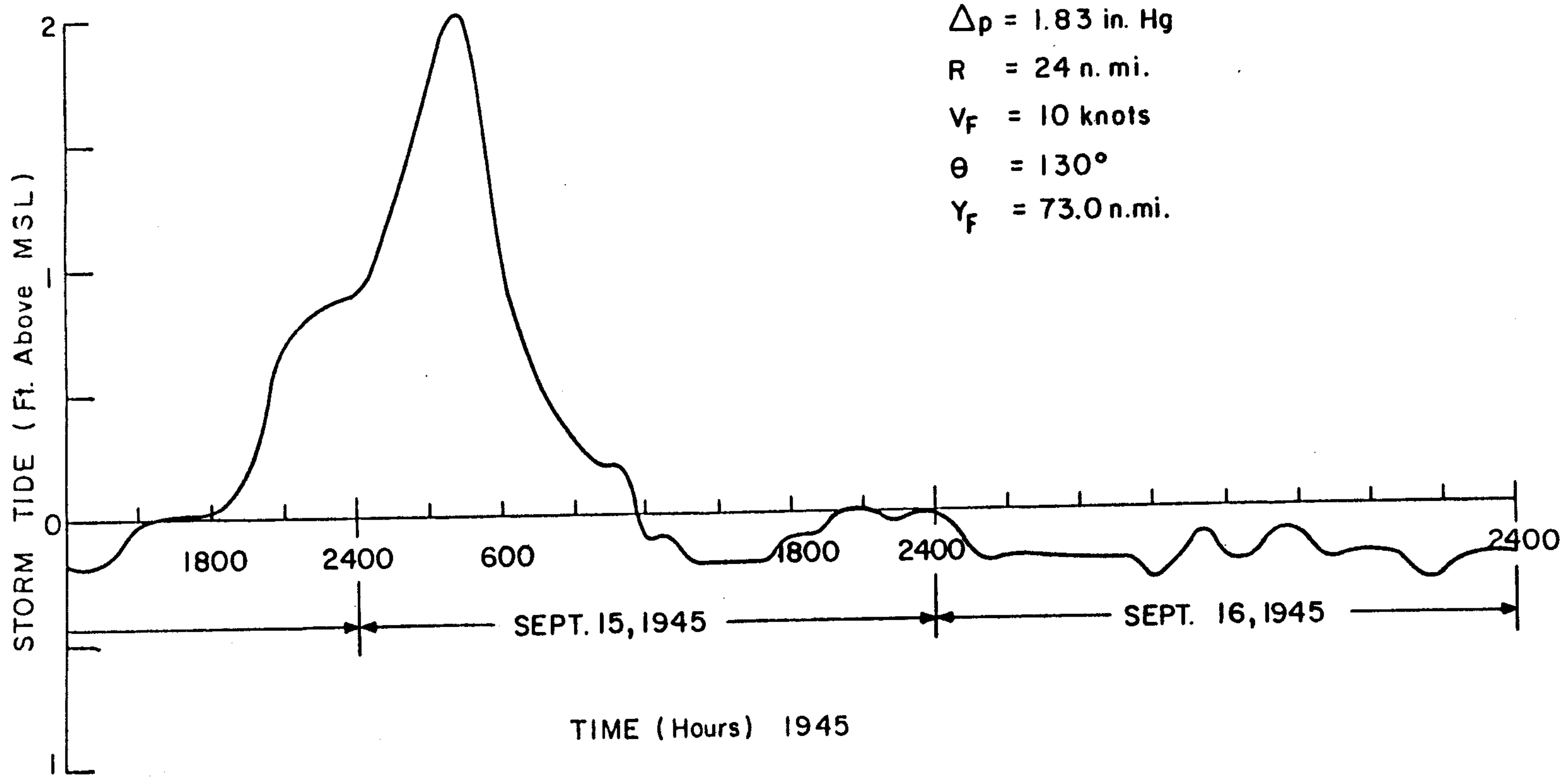

Figure 16. Storm Tide Generated by the 1945 Hurricane at Miami Beach (Recreation Pier)

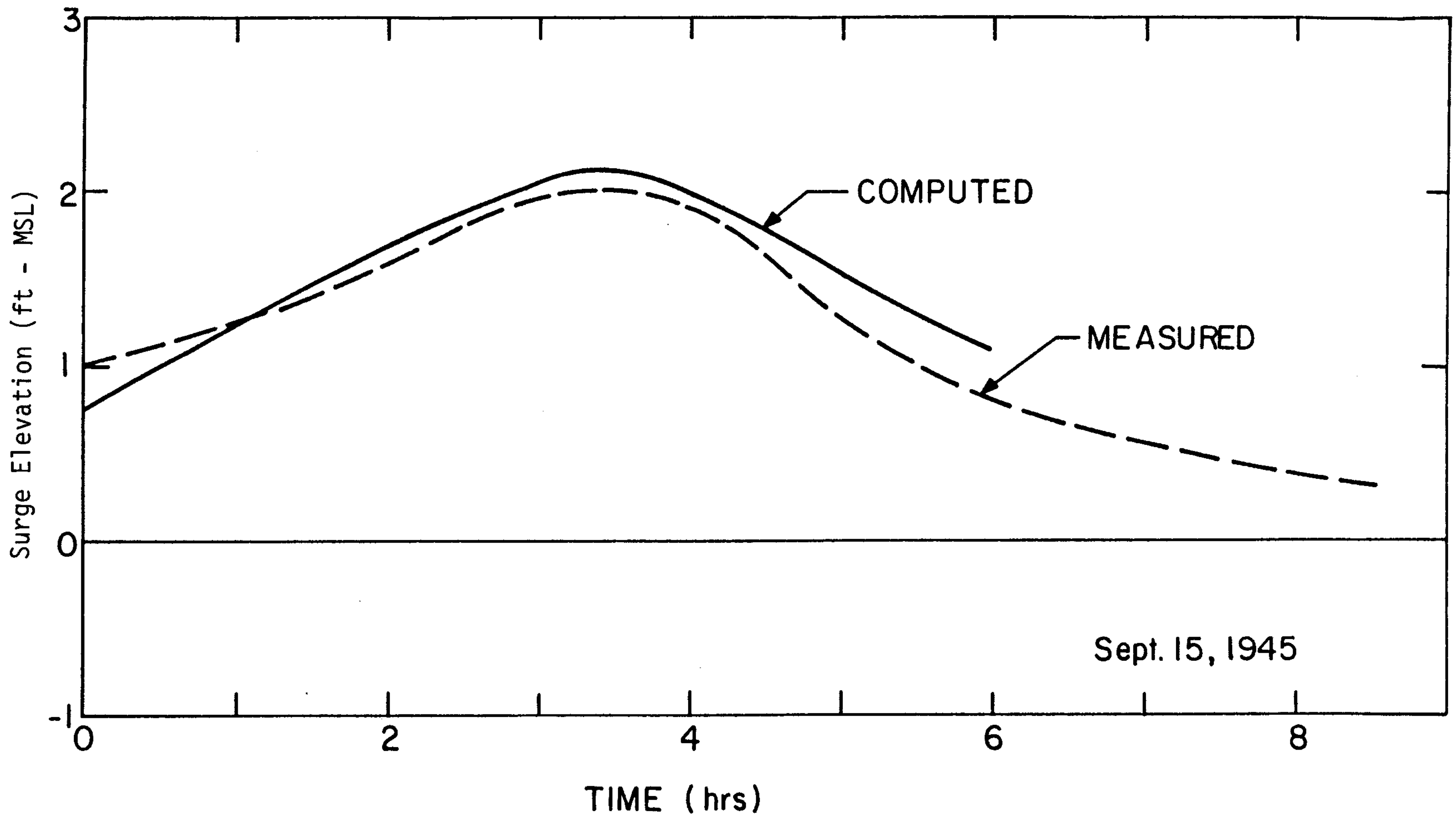

Figure 17. Comparison Between Measured and Computed Storm Peak Tides

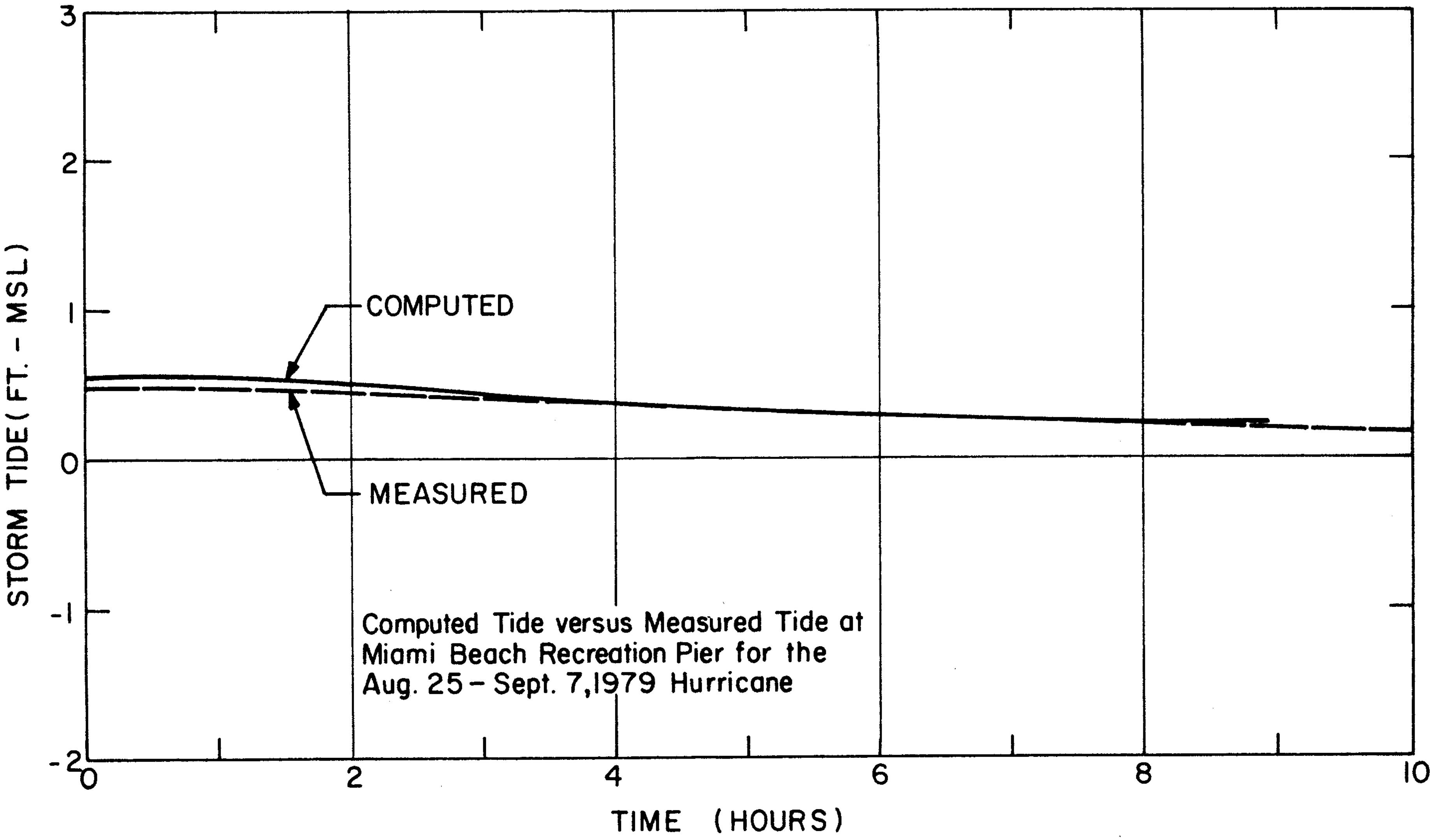

Figure 18. Comparison Between Measured and Computed Storm Peak Tides for August 25-September 7, 1979 Hurricane

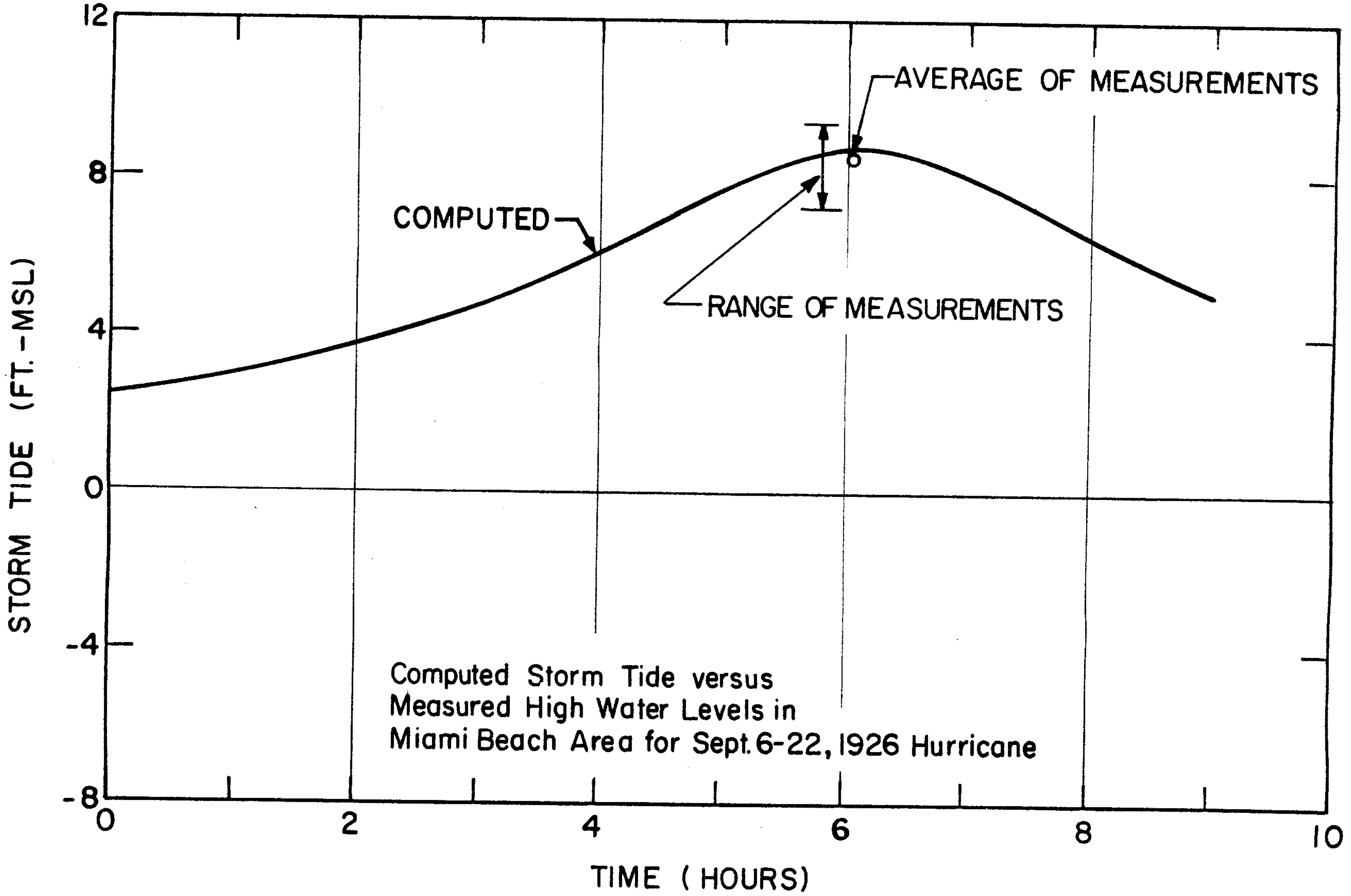

Figure 19. Comparison Between Measured and Computed Storm Peak Tides for September 17-21, 1926 Hurricane

5.3 Calibration of One-Dimensional Numerical Model

The 11 landfalling and 11 alongshore hurricanes are run using the two-dimensional model to establish the peak surge at the site. The characteristics of these hurricanes and the peak storm surges at the site are presented in Tables IIa and IIb.

A calibration relationship between the simple peak surges computed from the one-dimensional numerical model and those from the two-dimensional model is determined as follows. The peak surges computed from these two models are plotted as shown in Figure 20 for the landfalling storms. The relationship between the two computed values is thus represented by the straight line. For the alongshore storms, Figure 21 represents the straight line relationship for the north and middle profile and Figure 22 represents that for the south profile.

In summary, the overall calibration procedure for the simulation is that presented in Figure 14. Eleven landfalling storms and 11 alongshore storms with parameters encompassing representative ranges of their cumulative probability distributions are chosen. Peak storm surges corresponding to three locations along the Dade County shoreline (Figure 12) are calculated for the same 22 storms by both two-dimensional and one-dimensional numerical models. Then the calculated peak surges are correlated to establish the relationship between the one-dimesional and two-dimensional results. This "calibrated" storm surge relationship is then combined with dynamic wave setup and astronomical tide as described previously to establish a combined total storm tide. The peak of the combined total storm tide is the value at the site which is later ranked with 279 other similarly-determined peaks to establish the storm tides associated with various return periods of interest.

TABLE IIa

Parameters Defining 11 Storms Used in Calibrating the One-Dimensional Model with the Two-Dimensional Model

LANDFALLING STORMS

Model Storm	Δp (in. Hg)	R (n. mi.)	V_F (knots)	θ_N (degree)	Y_F (n. mi.)	η_{max} (ft) North Profile 2-D	North Profile 1-D	Middle Profile 2-D	Middle Profile 1-D	South Profile 2-D	South Profile 1-D	Starting Coordinates of Storm y_s	x_s
1	-1.5	25	10	100	35	1.78	1.76	1.86	1.77	1.83	1.78	37.1	50
2	-1.5	35	10	100	35	1.82	1.76	1.81	1.72	1.79	1.75	37.1	50
3	-1.5	15	10	100	35	1.55	1.59	1.83	1.85	1.96	1.82	37.1	50
4	-2.0	25	10	100	35	1.18	1.16	1.24	1.17	1.23	1.18	37.1	50
5	-1.0	25	10	100	35	2.40	2.35	2.50	2.36	2.45	2.38	37.1	50
6	-1.5	25	14	100	35	1.77	1.78	1.88	1.78	1.89	1.78	37.1	50
7	-1.5	25	6	100	35	1.78	1.73	1.86	1.75	1.80	1.78	37.1	50
8	-1.5	25	10	140	35	1.82	1.68	1.86	1.65	1.98	1.55	72.3	50
9	-1.5	25	10	60	35	1.79	1.60	1.84	1.80	2.17	2.64	4.9	50
10	-1.5	25	10	100	41	1.63	1.64	1.81	1.84	2.20	2.27	43.1	50
11	-1.5	25	10	100	29	1.83	1.74	1.77	1.66	1.68	1.54	31.1	50

TABLE IIb
Parameters Defining 11 Storms Used in Calibrating the One-Dimensional Model with the Two-Dimensional Model
ALONGSHORE STORMS

Model Storm	Δp (in. Hg)	R (n. mi.)	V_F (knots)	θ_N (degree)	X_L (n. mi.)	η_{max} (ft) North Profile 2-D	North Profile 1-D	Middle Profile 2-D	Middle Profile 1-D	South Profile 2-D	South Profile 1-D	Starting Coordinates of Storm y_s	x_s
1	-1.5	25	10	190	35	1.13	0.84	1.15	0.86	1.32	1.19	70	32.9
2	-1.5	30	10	190	35	1.25	0.95	1.27	0.97	1.45	1.34	70	32.9
3	-1.5	20	10	190	35	0.99	0.71	1.01	0.73	1.21	1.01	70	32.9
4	-2.0	25	10	190	35	1.52	1.12	1.55	1.16	1.79	1.63	70	32.9
5	-1.0	25	10	190	35	0.75	0.55	0.76	0.57	0.86	0.75	70	32.9
6	-1.5	25	14	190	35	1.10	0.83	1.12	0.85	1.26	1.17	70	32.9
7	-1.5	25	6	190	35	1.17	0.84	1.20	0.86	1.42	1.21	70	32.9
8	-1.5	25	10	200	35	1.14	0.87	1.20	0.93	1.47	1.38	70	25.8
9	-1.5	25	10	180	35	1.14	0.81	1.14	0.81	1.22	1.02	70	39.9
10	-1.5	25	10	190	45	0.92	0.70	0.93	0.71	1.01	0.95	70	42.9
11	-1.5	25	10	190	25	1.43	1.04	1.49	1.07	1.75	1.51	70	22.9

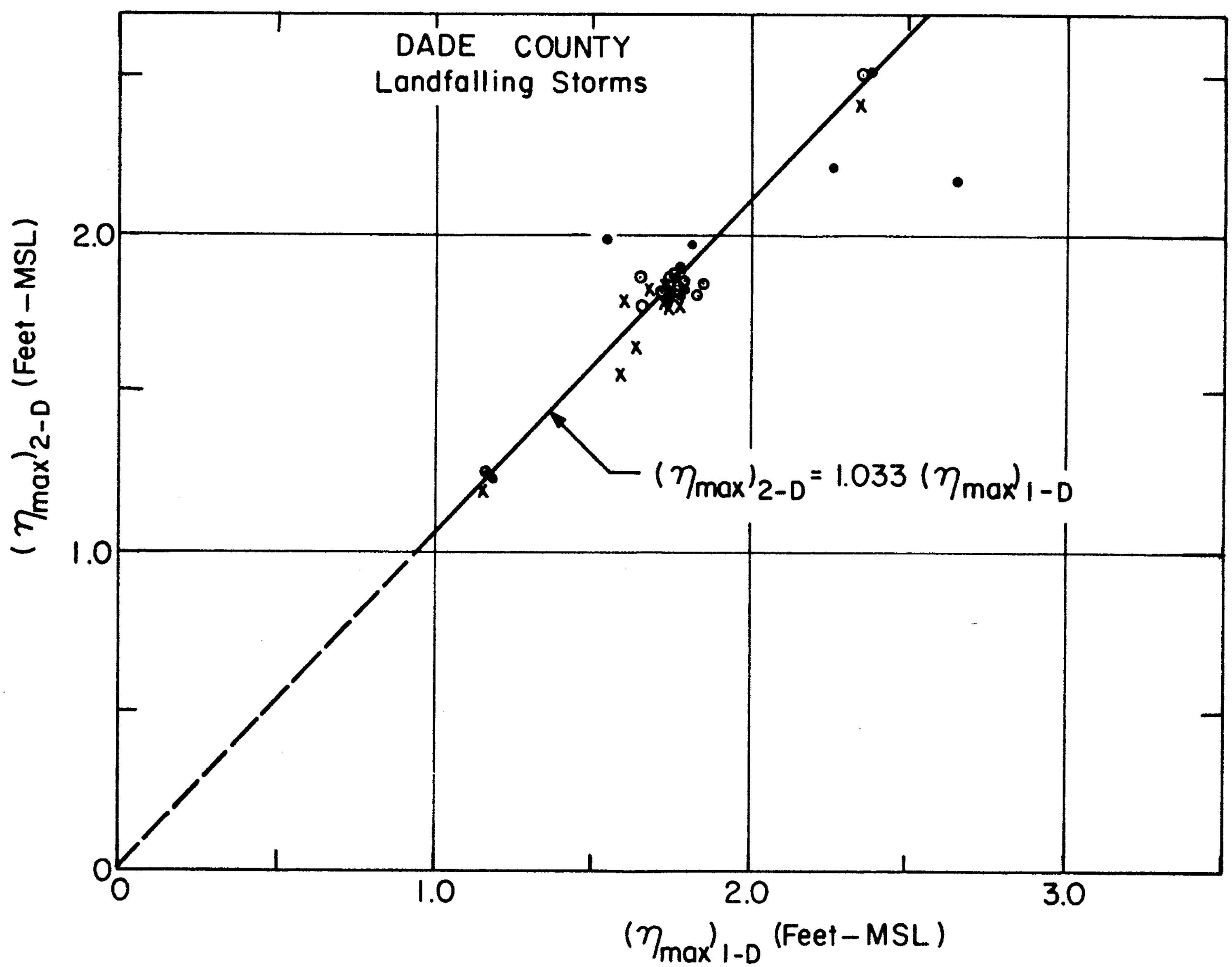

Figure 20. Comparison Between the One-Dimensional Calculations and the Two-Dimensional Calculations of Peak Surges at Three Locations Along Dade County Shoreline for 11 Landfalling Model Storms

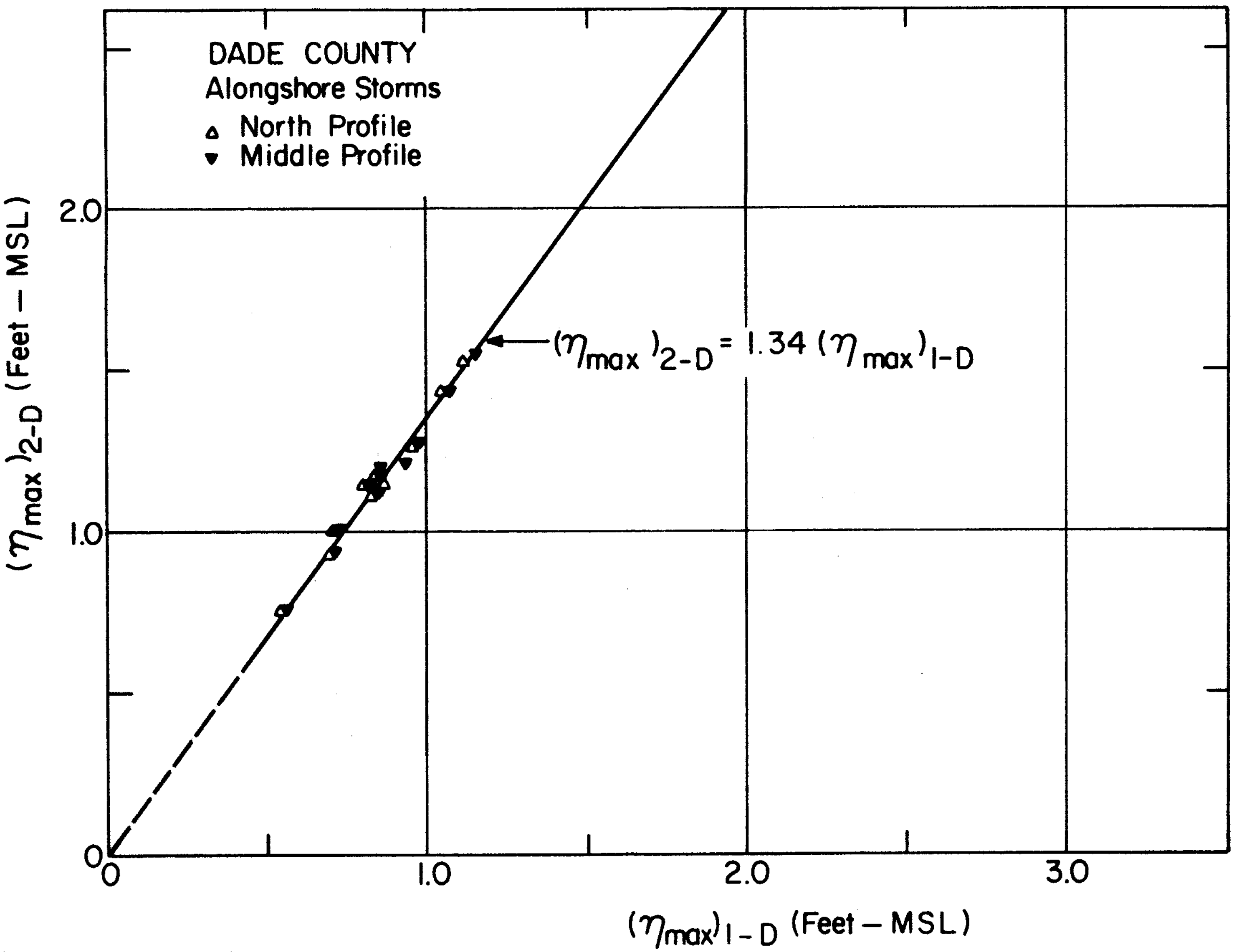

Figure 21. Comparison Between the One-Dimensional Calculations and the Two-Dimensional Calculations of Peak Surges at the North and Middle Location of Dade County Shoreline for 11 Alongshore Model Storms

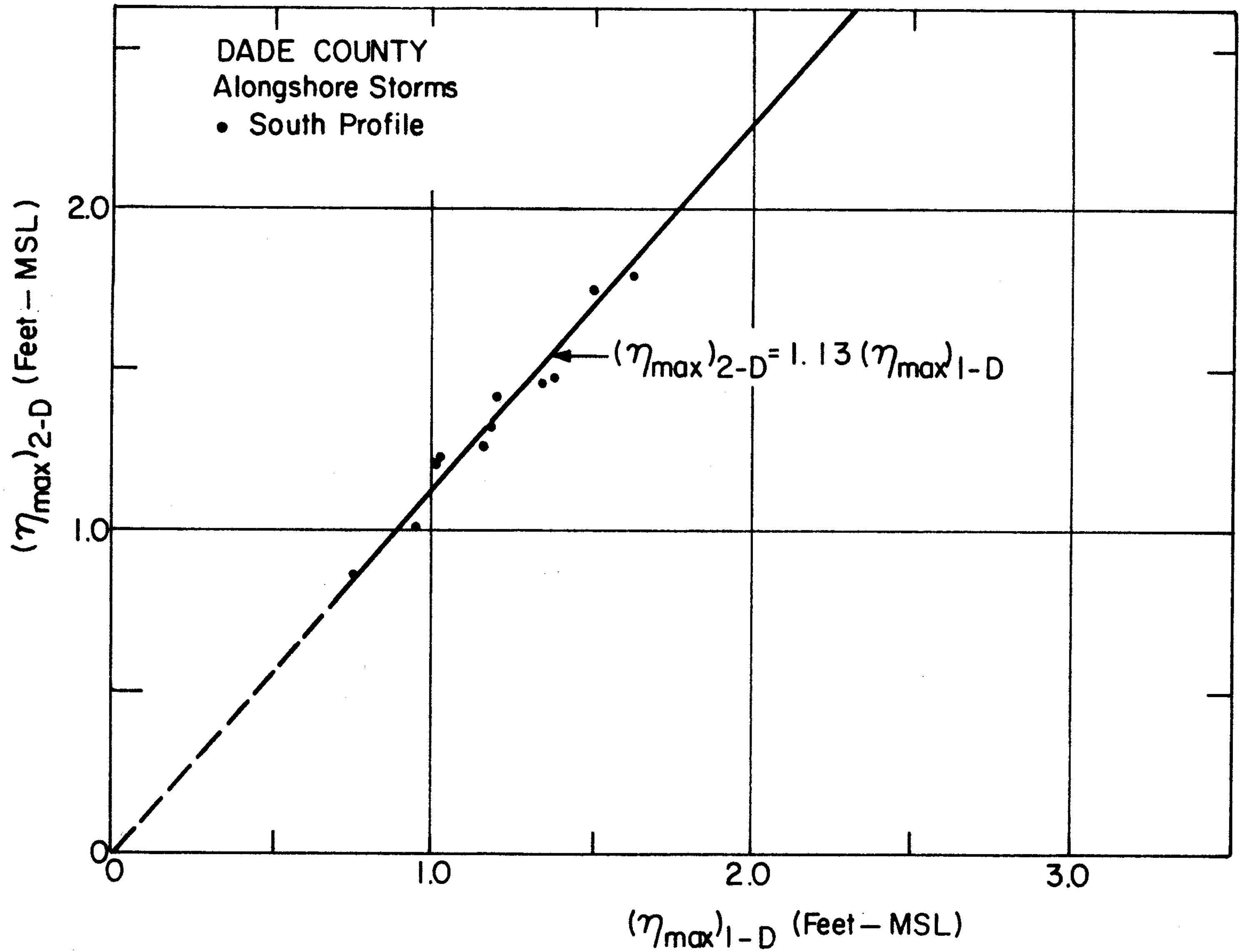

Figure 22. Comparison Between the One-Dimensional Calculations and the Two-Dimensional Calculations of Peak Surges at the South Location of Dade County Shoreline for 11 Alongshore Model Storms

VI. RESULTS OF LONG TERM SIMULATIONS

Three 500-year simulations for each one of the three locations are carried out employing the computer methods and hurricane statistics presented in the preceding sections. The combined total storm tides above local Mean Sea level and associated return periods computed from Eq. 22 are also presented. The results are plotted on semi-log paper in Figures 23a, 23b and 23c for the three locations along the Dade County shoreline. A line approximately representing the average value of the three simulations is adopted for each of the three locations along the Dade County shoreline. Figure 24 shows the north and south combined storm tide curves together. The middle tide curve is very close to the north curve and is not shown.

Table III below presents the combined total storm tide values and corresponding return periods.

TABLE III
Combined Total Storm Tide Values for Various Return Periods

Return Period, TR (years)	Combined Total Storm Tide Level* above MSL (ft)		
	North	Middle	South
500	17.6	17.7	18.0
200	15.3	15.4	15.8
100	13.5	13.6	14.0
50	11.4	10.8	12.1
20	9.3	9.5	9.8
10	8.0	8.1	8.2

*Includes contributions of: wind stress, barometric pressure, dynamic wave setup and astronomical tides.

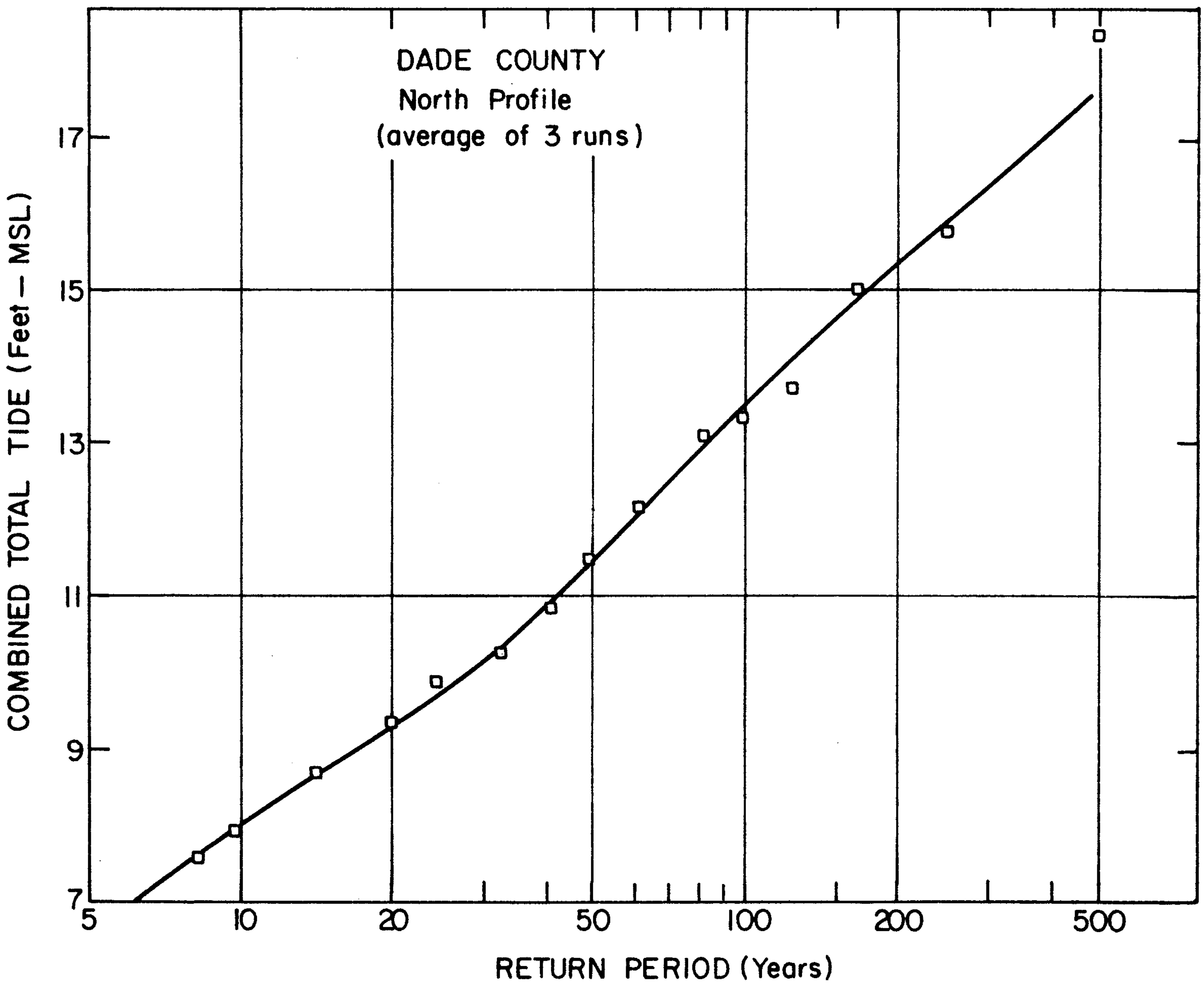

Figure 23a. Results of Three 500 Year Simulations for North Profile, Dade County

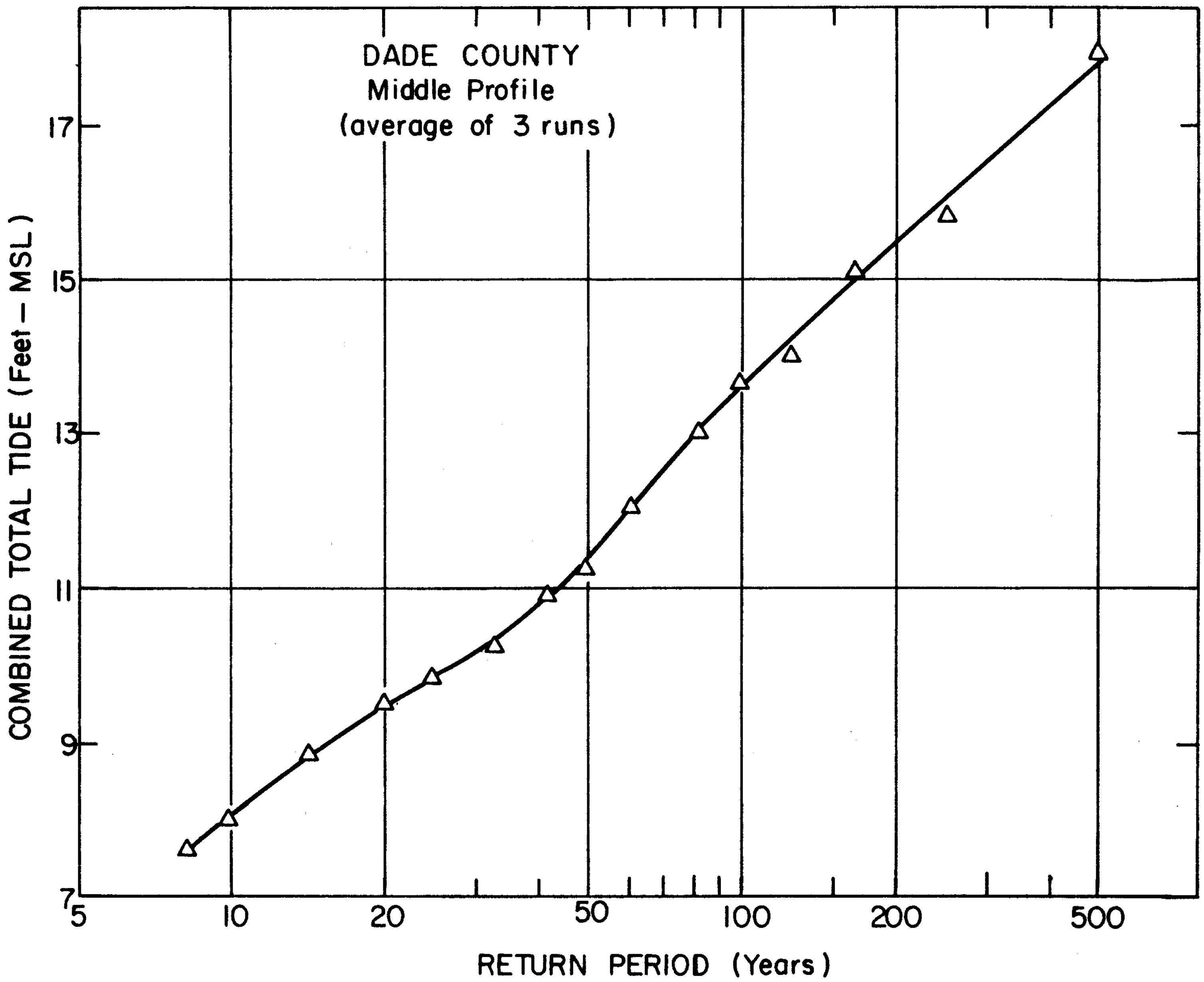

Figure 23b. Results of three 500 Year Simulations for Middle Profile, Dade County

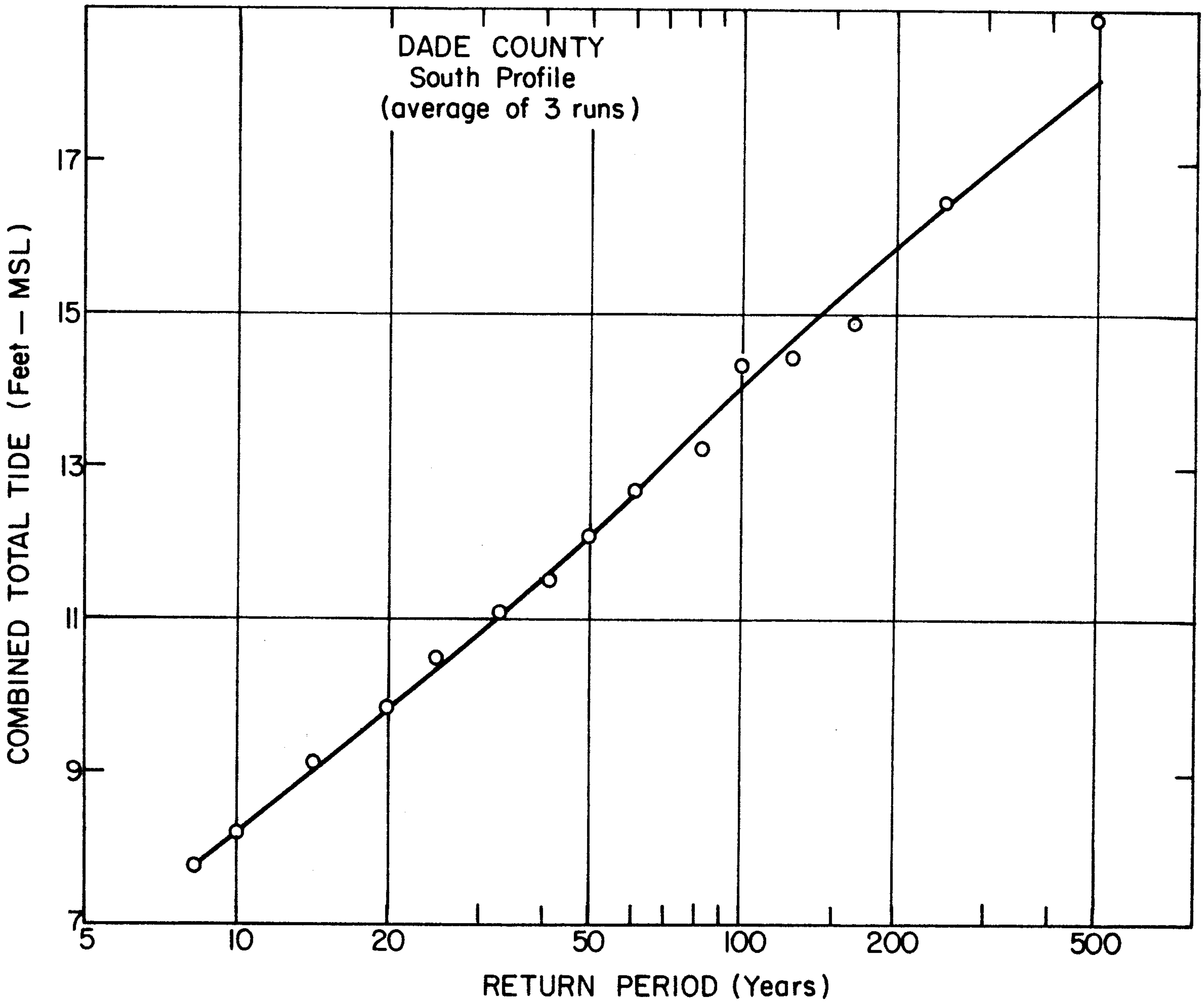

Figure 23c. Results of Three 500 Year Simulations for South Profile, Dade County

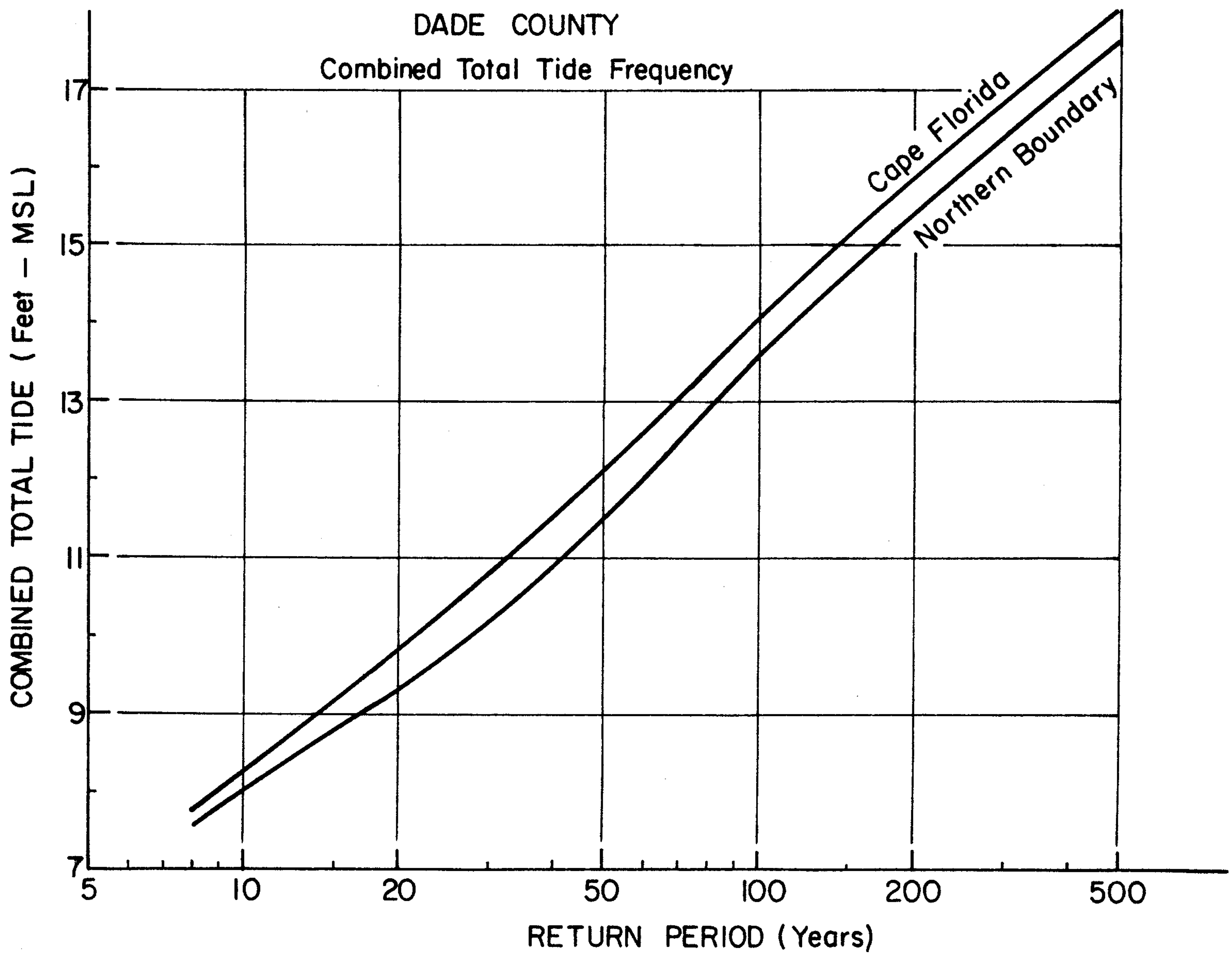

Figure 24. Combined Total Storm Tide Elevation Versus Return Period for Three Representative Profiles in Dade County

REFERENCES

1. Graham, H. E. and D. E. Nunn, "Meterological Considerations Pertinent to Standard Project Hurricane, Atlantic and Gulf Coasts of the United States," National Hurricane Research Report No. 33, U. S. Department of Commerce, November, 1959.

2. Ho, F. P., R. W. Schwerdt, and H. V. Goodyear, "Some Climatological Characteristics of Hurricanes and Tropical Storms, Gulf and East Coasts of the United States," National Weather Service, U. S. Department of Commerce, NOAA Technical Report NW515, May 1975.

3. National Oceanic and Atmospheric Administration, "Report-Flood Insurance Study-Broward County, Florida," June, 1972.

4. Wilson, B. L., "Hurricane Wave Statistics for the Gulf of Mexico," U. S. Army Corps of Engineers, Beach Erosion Board, Technical Memorandum 98, 1956.

5. Harris, D. L., "Characteristics of the Hurricane Storm Surge," Technical Paper No. 48, Weather Bureau, U. S. Department of Commerce, Washington, D. C., 1963.

6. Van Dorn, W., "Wind Stress on an Artificial Pond," Journal of Marine Research, Vol. 12, No. 3, 1953.

7. Christensen, B. A. and R. Walton, "Friction Factors in Flooding Due to Hurricanes," Proceedings, National Symposium on Urban Stormwater Mangement in Coastal Areas, Balcksburg, Virginia, June 19-20, 1980.

8. Saville, T., "Experimental Determination of Wave Set-up," Proceedings, Second Technical Conference on Hurricanes, 1961, p. 242-252.

9. Bowen, A. J., D. L. Inman and V. P. Simmons, "Wave 'Set-Down and Set-Up'," Journal of Geophysical Research, Vol. 73, NO. 8, 1968, p. 2569-2577.

10. Lo, J. M., "Surf Beat: Numerical and Theoretical Analysis," Ph.D. Dissertation, Department of Civil Engineering, University of Delaware, June, 1981.

11. U. S. Army Corps of Engineers, "Shore Protection Manual, Volumes I, II and III," U. S. Government Printing Office, 1977.

12. U. S. Army Corps of Engineers, Jacksonville District, "Preliminary-Examination Report on Hurricane-Protective Measures for Biscayne Bay, Fla.," Serial No. 50, January, 1958.

Appendix A

HURRICANE MODEL

The idealized hurricane model moving at a constant speed V_F at an angle, θ', with respect to the x-axis of the grid system is shown below. The gradient

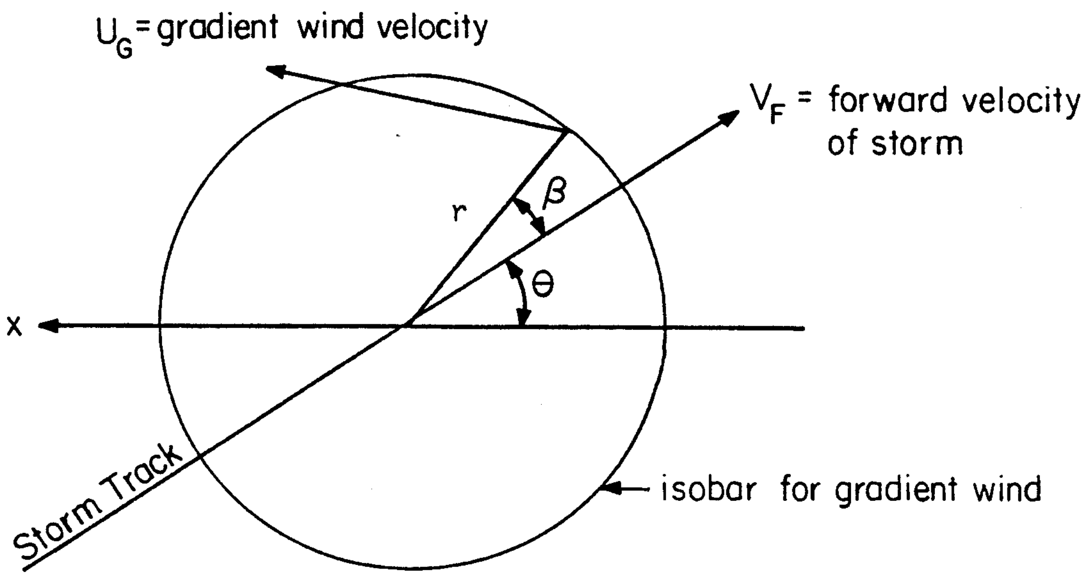

wind speed, U_G (wind speed at 30 ft. above water surface), is calculated by

$$U_G = U_c\ (\sqrt{\gamma^2 + 1} - \gamma) \cdot (0.83)$$

where

$$\gamma = \frac{1}{2}\left(\frac{V'}{U_c} + \frac{U_c}{U_g}\right)$$

and

$$U_c = \sqrt{\frac{\Delta p}{\rho_a} \frac{R}{r} e^{-R/r}}$$

$$U_g = \frac{\frac{\Delta p}{\rho_a} \frac{R}{r^2} e^{-R/r}}{2\omega(\sin \phi)}$$

$2\omega (\sin \phi)$ = coriolis effect

ω = earth rotation

ϕ = latitude

R = radius to maximum winds

$V' = V_F \sin \beta$

β = angle between observer and hurricane direction

V_F = constant translational speed of hurricane

ρ_a = mass density of air

r = distance from hurricane center to observer

U_g = geostrophic velocity component

U_c = cyclostrophic velocity component.

The factor of 0.83 was applied to the calculation of U_G to take into account friction effects at 30 feet above the water surface.